POLITECNICO DI TORINO

Collegio di Ingegneria Chimica e dei Materiali

Master of Science Course
Ingegneria Chimica e dei Processi Sostenibili

A.a 2025/26

Master of Science Thesis

PFAS Degradation and Fluorine Capture during Biosolids Pyrolysis

Tutors

Stefania Specchia
Silvia Fiore
Franco Berruti

Candidate
Antonino Maria Dattolo

Prefazione

Negli ultimi decenni la gestione sostenibile dei rifiuti derivanti dal trattamento delle acque reflue ha assunto un ruolo sempre più rilevante nelle politiche ambientali e nelle strategie di economia circolare. I biosolidi prodotti negli impianti di trattamento delle acque reflue rappresentano una risorsa potenzialmente valorizzabile grazie al loro contenuto di materia organica e nutrienti. Tuttavia, la presenza di contaminanti persistenti, in particolare i composti per- e polifluoroalchilici (PFAS), pone importanti sfide per il loro utilizzo sicuro e sostenibile.

I PFAS sono una vasta famiglia di sostanze chimiche sintetiche caratterizzate da un'elevata stabilità chimica dovuta al forte legame carbonio-fluoro. Questa caratteristica rende tali composti estremamente persistenti nell'ambiente e difficilmente degradabili nei processi convenzionali di trattamento delle acque reflue. Di conseguenza, i PFAS tendono ad accumularsi nei fanghi di depurazione e nei biosolidi prodotti dagli impianti di trattamento.

Negli ultimi anni la ricerca scientifica ha rivolto crescente attenzione allo sviluppo di tecnologie innovative per il trattamento dei biosolidi contaminati da PFAS. Tra queste, i processi termochimici e in particolare la pirolisi hanno attirato notevole interesse. La pirolisi consiste nella decomposizione termica della materia organica in assenza di ossigeno e produce tre principali frazioni: un residuo solido ricco di carbonio (biochar), una frazione liquida condensabile (bio-oil) e una frazione gassosa. Questo processo può contribuire alla riduzione del volume dei biosolidi e alla trasformazione o rimozione di contaminanti persistenti.

In questo contesto si inserisce la presente tesi, che analizza il comportamento dei PFAS durante la pirolisi dei biosolidi e valuta l'efficacia del processo nel ridurre la presenza di tali contaminanti. Lo studio si concentra in particolare sulla distribuzione dei PFAS e del fluoro associato tra le diverse frazioni di prodotto e sull'influenza delle condizioni operative del processo.

La ricerca è stata condotta utilizzando biosolidi provenienti da impianti di trattamento delle acque reflue e impiegando un reattore sperimentale operante in condizioni controllate. Sono stati analizzati diversi parametri di processo, tra cui la temperatura di pirolisi, il tempo di residenza dei solidi e l'aggiunta di additivi a base di calcio, al fine di valutare il loro effetto sulla degradazione dei PFAS e sulla distribuzione dei prodotti di pirolisi.

Il lavoro sperimentale è stato svolto nell'ambito del programma di mobilità internazionale Erasmus+, durante un periodo di ricerca trascorso in Canada presso l'Institute for Chemicals and Fuels from Alternative Resources (ICFAR) della Western University, situata a London, Ontario.

Capitolo I – Introduction

Il primo capitolo introduce il contesto generale in cui si inserisce il presente lavoro di ricerca, evidenziando le principali problematiche ambientali legate alla gestione dei biosolidi prodotti negli impianti di trattamento delle acque reflue. Con l'aumento della popolazione e dell'urbanizzazione, la quantità di fanghi di depurazione generati a livello globale è cresciuta in modo significativo, rendendo sempre più importante individuare strategie sostenibili per il loro trattamento e riutilizzo.

I biosolidi rappresentano infatti una matrice ricca di materia organica e nutrienti, e per questo motivo sono spesso utilizzati come ammendanti agricoli o fertilizzanti. Tuttavia, negli ultimi anni è emersa una crescente preoccupazione legata alla presenza di contaminanti persistenti all'interno di questi materiali. Tra questi contaminanti, un ruolo particolarmente rilevante è svolto dai composti per- e polifluoroalchilici (PFAS), una vasta classe di sostanze chimiche sintetiche caratterizzate da un'elevata stabilità chimica e ambientale.

I PFAS sono stati ampiamente utilizzati in numerosi prodotti industriali e di consumo grazie alle loro proprietà idrorepellenti e oleorepellenti. Tuttavia, la loro elevata persistenza nell'ambiente e la difficoltà di degradazione nei processi di trattamento convenzionali hanno portato alla loro diffusione in diverse matrici ambientali. Gli impianti di trattamento delle acque reflue non sono infatti progettati per rimuovere efficacemente questi composti, che tendono quindi ad accumularsi nei fanghi prodotti durante i processi di depurazione.

Il capitolo evidenzia inoltre come l'applicazione dei biosolidi in agricoltura possa rappresentare una possibile via di trasferimento dei PFAS nell'ambiente e nella catena alimentare. Questo aspetto ha portato a un crescente interesse scientifico verso lo sviluppo di tecnologie innovative in grado di ridurre o eliminare questi contaminanti dai biosolidi.

In questo contesto, i processi termochimici ad alta temperatura stanno emergendo come possibili soluzioni per il trattamento dei biosolidi contaminati. In particolare, la pirolisi rappresenta una tecnologia promettente in quanto consente la decomposizione termica della materia organica in assenza di ossigeno, producendo biochar, bio-olio e gas. Questa tecnologia potrebbe contribuire alla riduzione delle concentrazioni di PFAS nei biosolidi e alla valorizzazione dei prodotti ottenuti dal processo.

Il capitolo conclude introducendo gli obiettivi principali della tesi, che riguardano lo studio della degradazione dei PFAS durante la pirolisi dei biosolidi e la valutazione dell'influenza delle condizioni operative, come temperatura e tempo di residenza, sulla distribuzione dei prodotti e sulla rimozione dei contaminanti.

Capitolo II - PFAS: Background and Environmental Challenges

Il secondo capitolo fornisce una panoramica dettagliata delle caratteristiche chimiche, delle fonti e delle implicazioni ambientali dei composti per- e polifluoroalchilici (PFAS). Questi composti costituiscono una vasta famiglia di sostanze chimiche sintetiche sviluppate a partire dagli anni Cinquanta e utilizzate in numerosi prodotti industriali e commerciali grazie alle loro proprietà uniche di resistenza all'acqua, agli oli e alle alte temperature.

La struttura chimica dei PFAS è caratterizzata da una catena carboniosa parzialmente o completamente fluorurata e da un gruppo funzionale polare terminale. La presenza del legame carbonio-fluoro, uno dei legami più forti nella chimica organica, conferisce a queste molecole una straordinaria stabilità chimica e termica. Questa caratteristica rende i PFAS altamente resistenti ai processi di degradazione naturale, contribuendo alla loro persistenza nell'ambiente.

Il capitolo analizza inoltre la classificazione dei PFAS, distinguendo tra composti perfluoroalchilici e polifluoroalchilici, e tra sostanze polimeriche e non polimeriche. Particolare attenzione viene dedicata ai composti più studiati e diffusi, come l'acido perfluoroottanoico (PFOA) e il perfluorottano sulfonato (PFOS), che sono stati oggetto di numerose ricerche a causa della loro diffusione e dei potenziali effetti sulla salute.

Successivamente viene analizzato il comportamento ambientale dei PFAS, evidenziando la loro elevata mobilità e capacità di trasporto su lunghe distanze. Questi composti possono accumularsi negli ecosistemi e negli organismi viventi grazie alla loro tendenza a legarsi alle proteine presenti nei tessuti biologici. Numerosi studi hanno infatti dimostrato la presenza di PFAS in diversi organismi.

Il capitolo approfondisce inoltre i possibili effetti sulla salute umana associati all'esposizione ai PFAS. Studi epidemiologici hanno collegato l'esposizione a questi composti a diversi effetti avversi, tra cui alterazioni del sistema immunitario, disfunzioni tiroidee, effetti sullo sviluppo e un aumento del rischio di alcune patologie.

Infine, il capitolo discute la presenza dei PFAS nei biosolidi derivanti dagli impianti di trattamento delle acque reflue e analizza il quadro normativo internazionale relativo alla regolamentazione di queste sostanze. Nonostante i progressi compiuti negli ultimi anni nella regolamentazione dei PFAS, esistono ancora importanti lacune normative, in particolare per quanto riguarda la gestione dei biosolidi contaminati. Questo contesto evidenzia la necessità di sviluppare tecnologie di trattamento innovative in grado di ridurre la presenza di PFAS nelle matrici ambientali.

Capitolo III - Wastewater Treatment and Biosolids Production

Il terzo capitolo descrive il funzionamento degli impianti di trattamento delle acque reflue e i processi attraverso cui vengono generati i biosolidi. Gli impianti di depurazione delle acque reflue urbane sono sistemi complessi progettati per rimuovere contaminanti fisici, chimici e biologici dalle acque reflue prima della loro reimmissione nell'ambiente. Questi impianti utilizzano una serie di trattamenti sequenziali che includono processi preliminari, primari, secondari e, in alcuni casi, trattamenti avanzati o terziari.

Il capitolo descrive inizialmente le principali fasi del trattamento delle acque reflue. Il trattamento preliminare è finalizzato alla rimozione dei materiali grossolani e delle particelle pesanti attraverso operazioni come grigliatura e dissabbiatura. Successivamente, il trattamento primario consente la separazione dei solidi sedimentabili tramite processi di sedimentazione gravitazionale, che portano alla formazione del cosiddetto fango primario.

La fase di trattamento secondario si basa invece su processi biologici, nei quali microrganismi presenti nei sistemi a fanghi attivi degradano la materia organica disciolta presente nell'acqua reflua. Questa fase consente di ottenere un'ulteriore riduzione della domanda biochimica di ossigeno (BOD) e dei solidi sospesi. Durante questo processo viene prodotta una biomassa microbica che contribuisce alla formazione del cosiddetto fango secondario.

I fanghi prodotti nelle diverse fasi del trattamento vengono successivamente sottoposti a ulteriori processi di stabilizzazione, tra cui digestione anaerobica, compostaggio, essiccazione o trattamenti chimici. Il materiale risultante da questi processi stabilizzati prende il nome di biosolidi. Questi materiali possono essere utilizzati come fertilizzanti o ammendanti del suolo grazie al loro contenuto di nutrienti, tra cui azoto e fosforo.

Il capitolo analizza inoltre la composizione tipica dei biosolidi, che include una combinazione di materia organica, nutrienti, metalli in traccia e diversi contaminanti organici emergenti. Tra questi contaminanti figurano farmaci, microplastiche e composti perfluoroalchilici (PFAS), che tendono ad accumularsi nei biosolidi durante il trattamento delle acque reflue.

Infine, il capitolo esamina le normative e le linee guida relative alla gestione dei biosolidi in diversi contesti geografici, tra cui Stati Uniti, Europa e Canada. Viene evidenziato come, nonostante esistano regolamentazioni consolidate per alcuni contaminanti tradizionali, la regolamentazione dei PFAS nei biosolidi sia ancora limitata o in fase di sviluppo. Questo scenario rende necessario lo sviluppo di nuove strategie di trattamento per ridurre la presenza di tali contaminanti nei biosolidi destinati al riutilizzo o allo smaltimento.

Capitolo IV - Contaminated PFAS Biosolids Treatment Technologies

Il quarto capitolo analizza le principali tecnologie disponibili per il trattamento dei biosolidi contaminati da PFAS, con particolare attenzione ai processi termochimici. L'aumento delle preoccupazioni ambientali legate alla presenza di PFAS nei biosolidi ha infatti stimolato la ricerca di tecnologie in grado di ridurre o eliminare questi contaminanti prima della loro eventuale applicazione al suolo o del loro smaltimento.

Il capitolo introduce inizialmente i limiti dei metodi tradizionali di trattamento dei biosolidi, come digestione anaerobica, compostaggio e stabilizzazione chimica, che risultano generalmente inefficaci nella degradazione dei PFAS. A causa della loro elevata stabilità chimica, questi composti resistono infatti alla maggior parte dei processi biologici e chimici comunemente utilizzati negli impianti di trattamento.

Successivamente vengono presentate diverse tecnologie avanzate per la rimozione o la distruzione dei PFAS. Tra queste vengono discusse tecniche quali ossidazione elettrochimica, trattamenti al plasma, adsorbimento su materiali avanzati e processi termici ad alta temperatura. Tuttavia, molte di queste tecnologie presentano limitazioni legate ai costi operativi, alla complessità dei sistemi o alla difficoltà di applicazione su larga scala.

In questo contesto, i processi termochimici come incenerimento, gassificazione e pirolisi stanno emergendo come possibili soluzioni per il trattamento dei biosolidi contaminati. In particolare, la pirolisi è oggetto di crescente interesse poiché consente la decomposizione termica della materia organica in assenza di ossigeno, producendo biochar, bio-olio e gas di pirolisi.

Il capitolo descrive i principi fondamentali della pirolisi, analizzando i principali parametri operativi che influenzano il processo, tra cui temperatura, tempo di residenza e velocità di riscaldamento. Viene inoltre discusso il comportamento dei PFAS durante il trattamento termico e i possibili meccanismi di degradazione o volatilizzazione di questi composti.

Un ulteriore aspetto analizzato riguarda il ruolo degli additivi nel processo di pirolisi. In particolare, composti a base di calcio, come l'idrossido di calcio, possono favorire la cattura del fluoro, formando composti stabili come il fluoruro di calcio. Questo approccio può contribuire a ridurre la quantità di fluoro incorporata nella matrice carboniosa del biochar.

Infine, il capitolo presenta una panoramica delle diverse configurazioni di reattori utilizzati per la pirolisi dei biosolidi, evidenziando vantaggi e limitazioni di ciascun sistema.

Capitolo V - Research Context and Objectives

Il quinto capitolo definisce il contesto scientifico della ricerca e presenta gli obiettivi specifici della tesi. Nonostante il crescente interesse verso l'utilizzo della pirolisi come tecnologia per il trattamento dei biosolidi contaminati da PFAS, numerosi aspetti relativi al comportamento di questi composti durante il processo termico rimangono ancora poco compresi.

In particolare, la letteratura scientifica mostra risultati spesso contrastanti riguardo all'efficacia della pirolisi nella degradazione dei PFAS. Alcuni studi riportano elevate efficienze di rimozione a temperature relativamente moderate, mentre altri evidenziano una persistenza significativa di questi composti o la formazione di prodotti intermedi fluorurati. Queste differenze possono essere attribuite a vari fattori, tra cui le condizioni operative del processo, la configurazione del reattore e la composizione del materiale trattato.

Un ulteriore elemento di incertezza riguarda la distribuzione dei PFAS e del fluoro derivante da questi composti tra le diverse frazioni generate durante la pirolisi. In molti studi, infatti, l'attenzione si concentra principalmente sulla frazione solida, mentre le possibili trasformazioni e redistribuzioni dei PFAS nelle frazioni liquide e gassose sono ancora poco documentate.

Alla luce di queste lacune conoscitive, il presente lavoro di ricerca si propone di analizzare il comportamento dei PFAS durante la pirolisi dei biosolidi in condizioni controllate di laboratorio. Lo studio è stato progettato per valutare l'influenza di diversi parametri operativi, tra cui la temperatura di pirolisi e il tempo di residenza dei solidi, sulla degradazione dei PFAS e sulla distribuzione dei prodotti.

Inoltre, sono stati condotti esperimenti con biosolidi arricchiti artificialmente con PFOS e PFOA per valutare l'efficienza di rimozione dei PFAS in presenza di concentrazioni iniziali note. Sono stati inoltre testati additivi a base di calcio per analizzare il loro potenziale effetto sulla cattura del fluoro e sulla riduzione della sua incorporazione nella matrice carboniosa del biochar.

Gli obiettivi principali della tesi possono essere riassunti nei seguenti punti: valutare l'efficienza di degradazione dei PFAS durante la pirolisi dei biosolidi, analizzare la distribuzione dei prodotti di pirolisi e studiare il ruolo delle condizioni operative e degli additivi nel determinare il destino dei PFAS durante il processo.

Capitolo VI - Materials and Methods

Il sesto capitolo descrive i materiali utilizzati nello studio e le procedure adottate per la preparazione dei campioni destinati agli esperimenti di pirolisi. L'obiettivo principale di questa sezione è garantire la riproducibilità delle condizioni sperimentali e fornire una descrizione dettagliata delle operazioni preliminari effettuate sui biosolidi prima del trattamento termico.

I biosolidi utilizzati in questo studio provengono da impianti di trattamento delle acque reflue e sono stati forniti sotto forma di cake umido. Inizialmente sono stati raccolti quattro diversi campioni di biosolidi, che sono stati sottoposti a operazioni di essiccazione e macinazione al fine di ottenere un materiale più omogeneo e facilmente manipolabile. Successivamente è stata effettuata un'analisi prossimale per determinare il contenuto di umidità, materia volatile, carbonio fisso e ceneri.

Sulla base dei risultati ottenuti durante questa fase preliminare, due campioni di biosolidi con caratteristiche composizionali differenti sono stati selezionati per gli esperimenti di pirolisi e identificati come Feedstock A e Feedstock B. Questa scelta ha permesso di analizzare il comportamento dei PFAS in biosolidi con proprietà chimiche e contenuti di ceneri differenti.

Prima degli esperimenti, i campioni sono stati essiccati in forno a circa 90 °C per rimuovere l'umidità residua e successivamente macinati per ottenere una dimensione delle particelle più uniforme. La riduzione della granulometria è stata effettuata utilizzando un sistema di macinazione meccanica, evitando un'eccessiva produzione di calore che avrebbe potuto alterare le proprietà dei campioni.

Il capitolo descrive inoltre la preparazione degli additivi utilizzati negli esperimenti. In particolare, è stato utilizzato idrossido di calcio ($Ca(OH)_2$), aggiunto ai biosolidi in proporzioni specifiche per valutare il suo effetto sulla degradazione dei PFAS e sulla cattura del fluoro durante la pirolisi.

Infine, una parte importante del capitolo è dedicata alla procedura di spiking dei PFAS. In alcuni esperimenti, i biosolidi sono stati arricchiti artificialmente con PFOS e PFOA al fine di ottenere concentrazioni iniziali controllate di questi composti. Le soluzioni di PFAS sono state preparate utilizzando metanolo come solvente e successivamente mescolate ai biosolidi attraverso agitazione meccanica per garantire una distribuzione uniforme dei contaminanti all'interno della matrice solida.

Capitolo VII - Experimental Setup

Il settimo capitolo descrive in dettaglio l'apparato sperimentale utilizzato per condurre gli esperimenti di pirolisi dei biosolidi. Gli esperimenti sono stati eseguiti presso il laboratorio ICFAR (Institute for Chemicals and Fuels from Alternative Resources) utilizzando un reattore di pirolisi progettato per operare in condizioni controllate di temperatura e atmosfera.

Il sistema sperimentale è costituito da diverse unità operative che consentono l'alimentazione del materiale, il processo termico e la raccolta dei prodotti generati durante la pirolisi. Il biosolido viene introdotto nel reattore tramite un sistema di alimentazione a vite controllato elettronicamente, che permette di mantenere una portata costante del materiale durante l'esperimento.

Il reattore è un cilindro verticale riscaldato mediante un sistema a induzione che consente di raggiungere e mantenere temperature di esercizio elevate. Durante il funzionamento, il materiale viene miscelato da un agitatore meccanico e interagisce con un letto di char formatosi all'interno del reattore, che contribuisce a stabilizzare il processo e il tempo di residenza dei solidi.

Il sistema è progettato per operare in atmosfera inerte, mantenuta mediante un flusso continuo di azoto che impedisce la presenza di ossigeno all'interno del reattore. Questo è un requisito fondamentale per il corretto svolgimento del processo di pirolisi.

I prodotti generati durante la pirolisi vengono separati attraverso un sistema di condensazione e raccolta dei gas. I vapori prodotti nel reattore passano attraverso una serie di condensatori raffreddati, nei quali si separa la frazione liquida (bio-oil), mentre i gas non condensabili vengono convogliati verso un sistema di campionamento. Durante ogni esperimento, campioni di gas non condensabili vengono prelevati a intervalli di tempo prestabiliti (15, 30 e 45 minuti) per consentire l'analisi della composizione del gas prodotto nel corso della reazione.

Il capitolo descrive inoltre le procedure di avvio e spegnimento del sistema sperimentale, nonché le condizioni operative utilizzate durante gli esperimenti. Le prove di pirolisi sono state condotte a due temperature principali, 500 °C e 650 °C, con tempi di residenza dei solidi pari a 15 e 30 minuti. Ogni condizione sperimentale è stata replicata più volte al fine di garantire l'affidabilità e la riproducibilità dei risultati.

Capitolo VIII - Analytical Methods

L'ottavo capitolo descrive le metodologie analitiche utilizzate per caratterizzare i campioni e analizzare i prodotti generati durante la pirolisi. Le tecniche impiegate consentono di determinare la composizione dei biosolidi iniziali, le rese dei prodotti di pirolisi e la concentrazione dei PFAS nelle diverse matrici.

Una delle prime analisi effettuate è stata l'analisi prossimale dei biosolidi, utilizzata per determinare il contenuto di umidità, materia volatile, ceneri e carbonio fisso. Questa analisi è stata eseguita seguendo lo standard ASTM D1762-84, con alcune modifiche adattate alle esigenze sperimentali del laboratorio.

Per la caratterizzazione della fase gassosa prodotta durante la pirolisi è stato utilizzato un micro-gascromatografo (MicroGC). Questo strumento consente di determinare la composizione dei gas non condensabili, identificando specie come idrogeno, monossido di carbonio, anidride carbonica, metano e altri idrocarburi leggeri.

La determinazione delle concentrazioni di PFAS nei campioni solidi e liquidi è stata effettuata utilizzando la tecnica LC-MS/MS (cromatografia liquida accoppiata a spettrometria di massa tandem). Prima dell'analisi strumentale, i campioni sono stati sottoposti a procedure di estrazione e purificazione basate sul metodo EPA 1633, che prevede l'uso di solventi organici e di cartucce di estrazione in fase solida (SPE).

Il capitolo descrive inoltre i metodi utilizzati per il calcolo delle rese dei prodotti di pirolisi e per la determinazione dell'efficienza di rimozione dei PFAS. In particolare, sono stati sviluppati metodi di conversione delle concentrazioni di PFAS in equivalenti di fluoro, al fine di analizzare il bilancio del fluoro tra le diverse frazioni prodotte durante il processo

Capitolo IX – Results

Il nono capitolo presenta e discute i risultati ottenuti dagli esperimenti di pirolisi dei biosolidi. L'analisi dei risultati si concentra su diversi aspetti fondamentali, tra cui la distribuzione dei prodotti di pirolisi, la composizione della fase gassosa e il comportamento dei PFAS durante il processo.

I risultati mostrano che la temperatura di pirolisi rappresenta il parametro operativo più importante nel determinare la distribuzione dei prodotti. All'aumentare della temperatura da 500 °C a 650 °C si osserva una diminuzione della resa in char e un aumento della produzione di gas.

Anche il tempo di residenza dei solidi influisce sulla distribuzione dei prodotti, sebbene il suo effetto sia meno marcato rispetto alla temperatura. Tempi di residenza più lunghi favoriscono la formazione di gas a causa della maggiore conversione del materiale organico.

L'analisi della composizione dei gas ha mostrato che a temperature più elevate aumenta la produzione di idrogeno, monossido di carbonio e idrocarburi leggeri, mentre la frazione di anidride carbonica diminuisce.

Per quanto riguarda i PFAS, i risultati evidenziano un'elevata efficienza di rimozione durante la pirolisi. Le analisi mostrano che la maggior parte del fluoro derivante dai PFAS non rimane nella frazione solida, indicando che i composti fluorurati vengono in gran parte trasferiti in altre fasi del processo.

L'aggiunta di idrossido di calcio ha inoltre mostrato un effetto positivo sulla riduzione della quantità di fluoro trattenuta nel char, grazie alla formazione di composti inorganici stabili come il fluoruro di calcio.

Nel complesso, i risultati suggeriscono che la pirolisi rappresenta una tecnologia promettente per il trattamento dei biosolidi contaminati da PFAS, in grado di ridurre significativamente la presenza di questi composti nella frazione solida finale.

1 Introduction

The sustainable management of waste represents a critical challenge in an era of increasing urbanization and industrialization. Among the various categories of waste treated in wastewater treatment plants, biosolids emerge as a potentially usable but problematic resource, as they may contain persistent and hazardous contaminants such as PFAS (Perfluoroalkyl Substances).

PFAS are persistent synthetic chemicals widely utilized in industrial and consumer products. For over 50 years, PFAS have been widely used as fire retardants, oil and water repellents for e.g. in furniture and clothing water-proofing (Ahrens, 2011; Arvaniti & Stasinakis, 2015; Ateia et al., 2019). They are regarded as environmental pollutants and have been linked to various types of cancer, developmental toxicity, and immunotoxicity (Ramirez Carnero et al., 2021). The extensive use of these compounds has led to the contamination of wastewater and, subsequently, biosolids generated in wastewater treatment facilities. PFAS primarily bind to biosolids through hydrophobic and electrostatic interactions, with PFOS and PFOA being the most commonly detected compounds (Moodie et al., 2021).

Further, in 2009, the US EPA set a lifetime health advisory level (HAL) to an individual maximum of 70 ng/L (ppt) in drinking water for both PFOA and PFOS, excluding other PFAS types (Rodowa et al., 2020). Likewise, the Drinking Water Directive (2020/2184/EU) sets a limit of 100 ng/L for the sum of 20 PFAS compounds that can be accurately measured.

However, as exemplified by perfluorooctane sulfonate (PFOS), PFAS in recent years have been under increasing scrutiny and concern as environmental contaminants due to evidence of high persistency, long-range transport, bioaccumulation potential and/or toxicity (Jian et al., 2017; Houde et al., 2011; Sunderland et al., 2019; Barry et al., 2013; Ballesteros et al., 2017; Bach et al., 2015; de Voogt and Saez, 2006; Ghisi et al., 2019).

PFAS can be released from consumer products during their lifespan and discharged into wastewater, thus entering wastewater treatment plants (WWTPs). Most WWTPs generate sludge and biosolids in either physical or biological wastewater treatment processes, but they are not equipped or designed to remove some persistent pollutants such as PFAS, and thus can be pathways of PFAS to the environment (Allred et al., 2015; Alder & van der Voet, 2015; Gewurtz et al., 2013; Guerra et al., 2014; Lee et al., 2014; Navarro et al., 2018). High PFAS concentrations in sewage sludge and biosolids from WWTPs have been reported (Arvaniti & Stasinakis, 2015; Hamid et al., 2018; Gewurtz et al., 2013). Biosolids are nutrient- and energy-rich materials, and widely used as a fertilizer substitute and/or soil conditioner for carbon sequestration. In Canada more than 660,000 dry tonnes of biosolids are generated annually (Jin et al., 2018), and about 43 % of them are used in land applications (Wang et al., 2013). Therefore, there can be a risk of PFAS exposure to humans or wildlife from biosolids applications (Braunig et al., 2019).

Conventional biosolids treatment methods, including lime stabilization, digestion, thermal drying, and composting, have proven ineffective in destroying PFAS, posing challenges for biosolids management and reuse (Kundu, et al., 2021; Longendyke et al., 2022).

In response to regulatory pressures and the growing awareness of PFAS-related risks, the wastewater industry is exploring innovative technologies to reduce or eliminate these contaminants in biosolids. Among the emerging solutions, high-temperature thermal treatments have garnered significant interest, with incineration being the most extensively studied technique

However, incineration presents several drawbacks, including the destruction of carbon and nutrients valuable for agricultural applications and the release of toxic emissions. Consequently, alternative thermal treatment techniques such as pyrolysis and gasification are gaining increased attention.

The pyrolysis process decomposes carbonaceous materials, such as biosolids, in the absence of oxygen. Usually, a sweeping gas flow is provided in the pyrolysis process such as N_2. Biochar (solid), bio-oil (liquid) and pyrolysis gas are the three products that are generated from the pyrolysis of biosolids. The yield

distribution of these products depends on a number of parameters including the composition of biosolids, pyrolysis temperature, heating/energy transfer rate, and flow rate of the sweeping gas as well as the catalyst/additive if used.

This thesis investigates the thermal degradation of PFAS in biosolids through pyrolysis at 500°C and 650°C using feedstocks sourced from wastewater treatment plants. The study aims to evaluate the effectiveness of pyrolysis in reducing measurable PFAS concentrations while simultaneously producing biochar with potential applications as a soil amendment. The influence of residence time, set at 15 and 30 minutes, was examined using a vertically agitated reactor operating under continuous conditions and approximating a continuously stirred tank reactor once a stable bed of solids is established. Particular attention is given to the distribution of PFAS-derived fluorine across pyrolysis products, including biochar, pyrolysis oil, and non-condensable gases. Additionally, the effects of PFAS spiking and the addition of selected additives were investigated to better understand PFAS partitioning and the potential redistribution of fluorinated compounds during pyrolysis.

2 PFAS: Background and Environmental Challenges

2.1 Industrial Use and Sources of PFAS

Per- and polyfluoroalkyl substances (PFAS) are a class of synthetic chemicals widely used for their hydrophobic and lipophobic properties. Since the 1950s, PFAS have been incorporated into numerous consumer and industrial products including non-stick cookware, firefighting foams, waterproof clothing, and food packaging. Their exceptional chemical stability, primarily due to the strong carbon-fluorine (C-F) bond makes them resistant to thermal, chemical, and biological degradation (Ahrens, 2011; Arvaniti & Stasinakis, 2015). Compared with other bond energies, such as the carbon-oxygen single bond (358 kJ/mol), the carbon-fluorine bond (485 kJ/mol) exhibits markedly higher stability, contributing to the environmental persistence of PFAS (Jiang et al., 2023).

Despite their widespread use, comprehensive information regarding PFAS content in commercial products remains limited. Confidential formulations, non-intentional contamination during manufacturing, and the large diversity of PFAS chemistries complicate efforts to assess human exposure pathways and environmental release dynamics. Although targeted analytical approaches have begun to address this gap, they still capture only a portion of the PFAS currently in commerce (Balan et al., 2021).

Dewapriya et al. (2023) conducted an extensive review examining PFAS occurrence across a wide range of consumer products. As shown in Figure 2.1, their analysis revealed substantial variability in PFAS concentrations depending on product type. In particular, commercially available firefighting foams exhibited the highest total PFAS levels (0.1-11,031 ppm; mean 488 ppm), followed by industrial textile finishing agents (mean 302 ppm) and household chemicals (mean 208 ppm). These findings demonstrate that everyday consumer products can act as significant PFAS reservoirs, underscoring the need for improved monitoring, disclosure, and regulatory oversight.

Beyond consumer products, PFAS originate from a broader network of sources and environmental pathways, including manufacturing emissions, waste disposal, wastewater treatment, and atmospheric or hydrological transport. To contextualize these additional mechanisms, Table 2.1 summarises the major PFAS sources and pathways reported in the wider literature. This table synthesizes key concepts from a separate study to complement the understanding of PFAS environmental dissemination(Phillip, 2025).

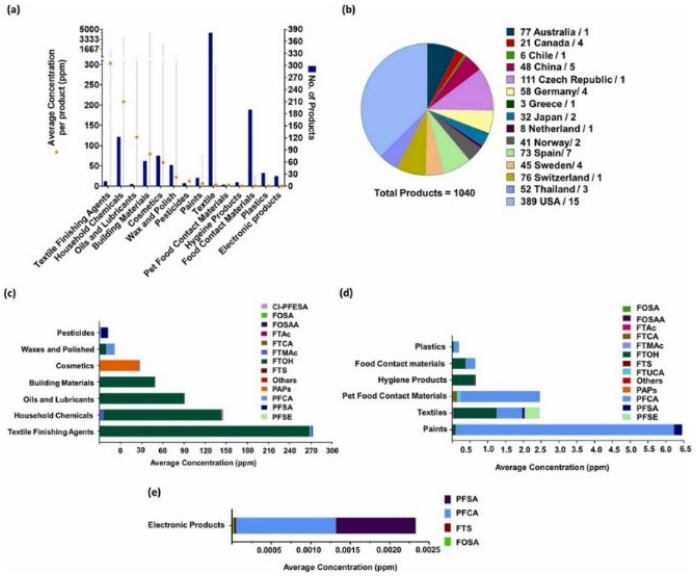

Figure 2.1 Summary of PFAS occurrence in consumer products (Dewapriya et al., 2023). **(a)** reports the average PFAS concentrations and the number of analyzed products for each product category. **(b)** shows the geographical distribution of the 1,040 products included in the review.**(c)** and **(d)** present the average concentrations of different PFAS classes across major product groups. **(e)** illustrates the PFAS composition in electronic products

Table 2.1 Overview of major PFAS sources and enviromenal dispersion pathways. Adapted from Phillip(2025)

Category	Subcategory	Description	Examples	References
Industrial and commercial sources	Manufacturing processes	PFASs are synthesized for the production of fluoropolymers via processes such as electrochemical fluorination. Their unique stability makes them ideal for high-performance applications.	PTFE production; mixture containing PFOA/PFOS	Mu et al., 2022; Kurwadkar et al., 2022
	Consumer products	PFASs are incorporated into many common goods to provide water, oil, and stain resistance.	Nonstick cookware; textiles; carpets; packaging.	Dewapriya et al., 2023
Firefighting foams	Military and airport settings	Aqueous film-forming foams (AFFF) containing PFAS are used to rapidly suppress high-intensity fuel fires in critical settings.	Military bases; airports; industrial areas.	Malik et al., 2024; Jahura et al., 2024
Waste management and discharge	Landfills	Discarded PFAS-treated consumer products eventually accumulate in landfills where PFAS can leach into adjacent soil and groundwater.	Nonstick cookware, textiles, and paper products; persistence in landfills due to resistance to degradation under typical conditions.	Coffin et al., 2023
	Wastewater treatment plants	PFAS enter municipal wastewater through domestic and industrial effluents, resulting in their discharge into water bodies.	PFAS appear in treated wastewater and accumulate in sludge, which may later be used as fertilizer,reintroducing PFAS into the environment.	Kurwadkar et al., 2022

2.2 Chemical Structure and Classification of PFAS

Per- and polyfluoroalkyl substances (PFAS) are a broad class of synthetic organic compounds characterized by the presence of a hydrophobic alkyl chain, typically comprising between 4 and 16 carbon atoms, in which hydrogen atoms are partially or fully replaced by fluorine. This fluorinated carbon backbone, coupled with a terminal polar functional group, imparts unique physicochemical properties such as thermal stability, chemical resistance, and surfactant behavior (AESAN).

The classification of PFAS depends largely on the degree of fluorination of the carbon chain. When all hydrogens on the carbon chain (except those on functional groups) are replaced by fluorine, the compound is termed a perfluoroalkyl substance. In contrast, polyfluoroalkyl substances are only partially fluorinated, but they can degrade or transform into perfluoroalkyl analogs under environmental or metabolic conditions

Structurally, PFAS can also be grouped into two broad categories: **non-polymeric PFAS**, which include substances like perfluorocarboxylic acids (PFCAs) and perfluorosulfonic acids (PFSAs), and polymeric PFAS, such as fluoropolymers and side-chain fluorinated polymers. Among the non-polymeric group, long-chain compounds like perfluorooctanoic acid (PFOA) and perfluorooctane sulfonic acid (PFOS) have been the most extensively studied due to their widespread occurrence and persistence in the environment(Figure 2.2-2.3).

To date, more than 4,500 compounds fall under the PFAS umbrella, but only a limited number have been the subject of detailed toxicological assessment and regulatory control. Most PFAS are acidic in nature and can exist in both protonated and anionic forms. While the terminology used to describe these compounds varies, it is generally recommended to refer to them collectively as “acids” rather than specifying individual forms such as carboxylates or sulfonates.(Schaider et al., 2017; Buck et al., 2011)

Due to their persistence and potential for bioaccumulation, PFAS are increasingly recognized as environmental contaminants of emerging concern, with some members of the class, particularly long-chain PFAS, linked to adverse health outcomes including immunotoxicity, endocrine disruption, developmental effects, and increased risk of certain cancers

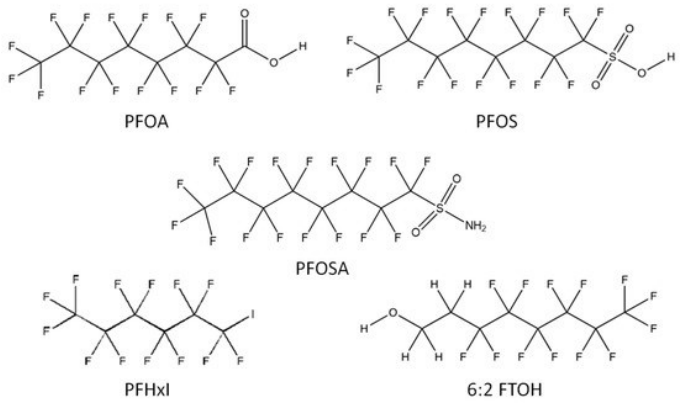

Figure 2.2 Chemical structure of selected PFAS. Source: Ramirez Carnero et al., 2021.

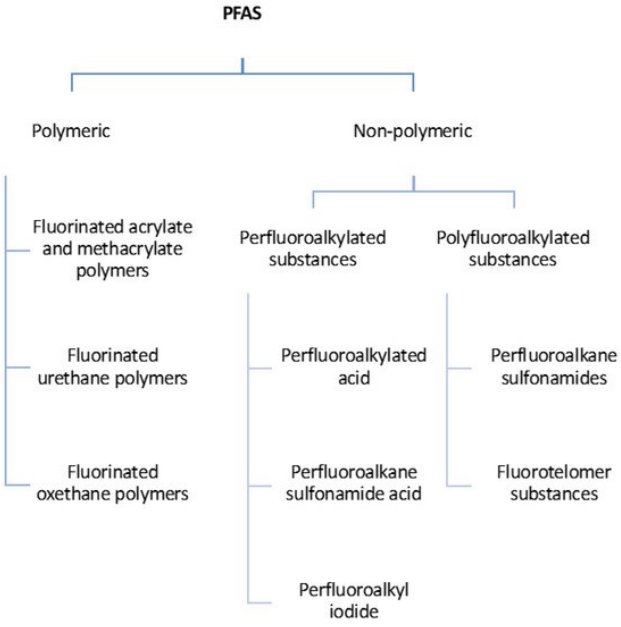

Figure 2.3 Schematic classification of PFAS. Source: Buck et al., 2011.

2.3 Enviromental Persistence and Enviromental Accumulation

PFAS exhibit a pronounced bioaccumulation potential, largely due to their strong proteinophilicity, which promotes binding to serum and tissue proteins and enhances their biological persistence. This interaction supports the accumulation of PFAS in various organs, including the liver, kidneys, and heart (Ng et al., 2013). Long-chain PFAAs are particularly prone to bioaccumulation, as they undergo minimal metabolic transformation and exhibit slow renal elimination, leading to prolonged retention compared with short-chain analogues (Müller et al., 2016). In aquatic ecosystems, PFAS protein interactions in water and sediment increase their bioavailability and facilitate trophic transfer. Consequently, elevated PFAS concentrations are frequently observed in higher trophic-level organisms, including apex predators such as polar bears and humans (Evich et al., 2022).

The environmental behavior of PFAS is further shaped by their dissociation constant (pKa), which governs their degree of ionization under typical environmental pH conditions. Reported pKa values for PFAS, such as -0.2 to 3.8 for PFOA indicate that most compounds predominantly exist in their anionic form (Vierke et al., 2013). Ionization status influences solubility, mobility, and interactions with soil and sediment matrices, thereby affecting environmental transport.

Sorption processes, commonly described by the soil-water partition coefficient (Kd), also play a major role in determining PFAS retention in soils. Longer-chain PFAS generally exhibit stronger sorption affinities due to increased hydrophobicity and larger molecular size (Nguyen et al., 2020). Soil pH is also a critical factor: under acidic conditions, reduced negative charge on soil organic matter enhances the sorption of anionic PFAS by decreasing electrostatic repulsion. Additional contributions from surface complexation with neutral organic and mineral phases further modulate retention (Meegoda et al., 2020).

Taken together, the persistence, bioaccumulation, and transport behavior of PFAS arise from the combined influence of their chemical stability, amphiphilic nature, ionization properties, and variable sorption affinities. These characteristics contribute to their widespread environmental distribution and highlight the challenges associated with their removal and remediation.

2.4 Health Impacts and Toxicological Concerns

Food consumption has recently emerged as one of the primary pathways of human exposure to PFAS (DeLuca et al., 2022; Eze et al., 2024; Holder et al., 2024; Roth et al., 2020). Consequently, recent research has increasingly focused on quantifying PFAS concentrations in foodstuffs and assessing dietary intake, particularly for well-studied compounds such as perfluorooctane sulfonic acid (PFOS) and perfluorooctanoic acid (PFOA), given their high exposure potential and toxicological relevance (Domingo & Nadal, 2017; EFSA CONTAM Panel, 2020; U.S. FDA, 2025).

Growing awareness of PFAS-related health and environmental risks underscores the need for continuous monitoring and updated dietary-exposure assessments. Among food categories, marine organisms exhibit the highest PFAS burdens, followed by livestock-derived products and plant-based foods, with PFOS and PFOA consistently reported as the predominant analytes (Langberg et al., 2024).

Numerous epidemiological and toxicological studies have associated PFAS exposure with adverse health effects. These include developmental toxicity, immune suppression, liver damage, thyroid dysfunction, and increased risk of certain cancers (Barry et al., 2013; Steenland et al., 2010; Ramirez Carnero et al., 2021). Due to these concerns, regulatory agencies such as the U.S. Environmental Protection Agency (EPA) and the European Union have issued health advisory levels for certain PFAS in drinking water (EPA, 2009; EU Directive 2020/2184).

2.5 Occurrence of PFAS in Wastewater Sludge and Biosolids

During wastewater treatment, PFAS are not fully removed and tend to partition into the solid phase via hydrophobic and electrostatic interactions. Consequently, high concentrations of PFAS are often found in sewage sludge and biosolids (Hamid et al., 2018; Arvaniti & Stasinakis, 2015). Conventional treatment processes such as anaerobic digestion, composting, and lime stabilization are largely ineffective in degrading these compounds (Kundu et al., 2021; Longendyke et al., 2022).

2.6 Regulatory Framework and Treatment Challenges

In response to growing environmental and public health concerns, regulatory bodies have begun to establish limits for PFAS, particularly in drinking water. For example, the U.S. EPA set a lifetime health advisory level of 70 ng/L for PFOA and PFOS in drinking water (EPA, 2009), while the EU adopted a 100 ng/L combined limit for 20 PFAS compounds (EU Directive 2020/2184). However, there is still a lack of comprehensive regulations for PFAS in biosolids. This regulatory gap, combined with the inefficacy of traditional treatment methods, has prompted increasing interest in advanced thermal technologies, such as pyrolysis, as a promising strategy for PFAS destruction or immobilization (Guerra et al., 2014; Bach et al., 2015).

3 Wastewater Treatment and Biosolids Production

3.1 Overview of Wastewater Treatment Plants

Municipal wastewater treatment plants (WWTPs) are complex, highly engineered systems whose purpose is to remove contaminants from sewage and industrial effluents. These systems rely on a series of physical, biological, and chemical treatments to reduce the concentrations of organic matter (quantified as biochemical oxygen demand, BOD, and chemical oxygen demand, COD), suspended solids, nutrients like nitrogen and phosphorus, and pathogenic organisms. The ultimate goal is to produce a treated effluent that is safe for discharge into the environment or suitable for reuse (Tchobanoglous et al., 2013; Metcalf and Eddy, 2003).

The treatment process in a typical WWTP is divided into a number of sequential stages, each designed to progressively remove different classes of pollutants.

The first of these stages is known as preliminary treatment, where the focus is on the removal of coarse materials that could damage equipment or interfere with downstream processes. This involves mechanical screening, which filters out large objects such as plastics and rags, followed by grit removal, which eliminates heavy inorganic particles like sand. In some plants, a flow equalization basin may be included to buffer fluctuations in water volume and organic load, helping to stabilize the performance of later stages (Henze et al., 2008).

Once these large and abrasive solids are removed, the water proceeds to primary treatment, where the primary goal is to separate settleable solids from the liquid stream through gravity. The wastewater flows into primary sedimentation tanks, allowing solids to settle to the bottom, forming what is known as primary sludge. This process typically results in the removal of 50-70% of total suspended solids (TSS) and about 25-40% of the BOD originally present in the influent. The next stage is secondary treatment, which relies on biological processes to degrade and remove dissolved and colloidal organic matter. The most commonly used technology here is the activated sludge process, where microorganisms in aeration tanks metabolize organic pollutants. The mixture then passes through secondary clarifiers, which separate the biomass from the treated water. Other biological systems used include trickling filters**,** sequencing batch reactors (SBRs)**,** and membrane bioreactors (MBRs). Collectively, secondary treatment can achieve over 85% removal of both BOD and TSS and may also contribute to partial nutrient removal, particularly nitrogen (Metcalf and Eddy, 2003).

In situations where higher treatment levels are required either to meet strict regulatory discharge limits or to enable water reuse **a** tertiary or advanced treatment stage is added. This phase can involve nutrient removal, either through chemical precipitation using compounds like ferric chloride or alum, or through biological processes designed to remove nitrogen and phosphorus. Additional processes include filtration**,** using media such as sand or membranes, and disinfection, typically achieved through chlorination**,** ozonation, or ultraviolet (UV) irradiation. In cases where the effluent contains persistent or hazardous micropollutants such as pharmaceuticals or PFAS, advanced oxidation processes (AOPs) which combine powerful oxidants like ozone or hydrogen peroxide with UV light may be employed (Andreozzi et al., 1999).

Together, these treatment stages transform raw wastewater into effluent that meets environmental standards, while also generating a substantial amount of sludge a byproduct that must be further treated and managed. The handling of this sludge, leading to the generation of biosolids, is addressed in the following section.

To provide a visual overview of the treatment stages described above, Figure 3.1 illustrates a typical municipal wastewater treatment plant, from raw sewage collection to effluent discharge and solids processing. The diagram highlights the sequential liquid-treatment operations screening, grit removal, primary clarification, biological treatment, and disinfectionas well as the solids-handling train, where primary and secondary sludge are thickened, digested, dewatered, and ultimately converted into biosolids. This schematic helps contextualize the specific points in the process where biosolids are generated and subsequently managed.

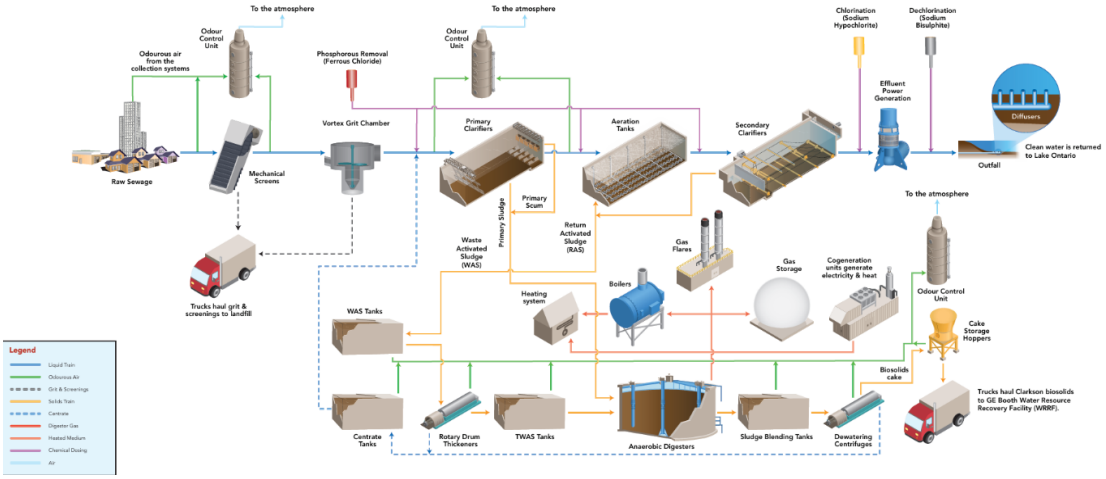

Figure 3.1 Schematic representation of a conventional municipal wastewater treatment plant, showing the sequential liquid-treatment processes (screening, grit removal, primary clarification, biological treatment and disinfection) and the associated solids-handling train, where primary and secondary sludge are thickened, digested and dewatered to produce biosolids.

3.2 Sludge Treatment and Biosolids Generation

Historically, wastewater was managed using *sewage farms*, large tracts of land where wastewater was applied to soil for natural filtration and nutrient removal. As urban populations expanded, these systems became impractical, leading to the development of more efficient technologies that required significantly less land. The introduction of engineered primary and secondary biological treatment in the early twentieth century progressively eliminated the need for sewage farms.

Modern wastewater treatment relies on a sequence of physical, chemical, and biological processes designed to separate solids from the liquid phase. Raw sewage typically moves through several treatment stages that, depending on the plant configuration, include primary, secondary, and in some cases tertiary treatment. During primary treatment, settleable and floatable solids are removed by sedimentation. In secondary treatment, often based on the activated sludge process, biodegradable dissolved and colloidal organic matter is oxidized and converted into microbial biomass.

The solids removed during these stages (i.e., primary and secondary sludge) are commonly processed through anaerobic digestion, where putrescible organic matter is converted into more stable compounds. The stabilized solids that result from digestion are referred to as *biosolids*, *sewage biosolids*, or simply *sludge*. Depending on regulatory requirements and the intended end use, biosolids may undergo further treatment such as dewatering, heat drying, composting, lime stabilization, or other processes to reduce pathogens, minimize odors, and improve handling characteristics (Apedaile, 2001; Metcalf & Eddy, 2003).

The Water Environment Federation (WEF) formally recognized the term *"biosolids"* in 1991 to distinguish biologically stabilized organic materials from untreated sewage sludge. To qualify as biosolids, sewage sludge must undergo sufficient treatment to reduce pathogens, odors, and vector attraction. A wide range of stabilization processes including anaerobic or aerobic digestion, composting, lime treatment, pasteurization, thermal hydrolysis, thermal drying, and air or solar drying may be used to achieve these criteria (Elgarahy et al., 2024).

Although the terms *sludge* and *biosolids* are often used interchangeably in informal contexts, the U.S. Environmental Protection Agency (EPA) uses the term *biosolids* specifically for sewage sludge that meets the treatment and quality requirements defined in the Standards for the Use or Disposal of Sewage Sludge (40 C.F.R. Part 503). Biosolids that comply with these standards may be applied to land as soil conditioners or fertilizers (EPA).

3.3 Typical Composition and Contaminants in Biosolids

Biosolids are heterogeneous materials whose composition depends on the characteristics of the influent wastewater, the presence of domestic and industrial discharges, and the treatment and stabilization methods applied within wastewater treatment plants. Their composition combines organic matter, nutrients, inorganic minerals, and a variety of trace contaminants that are either naturally present or introduced through anthropogenic activity.

3.3.1 Organic Matter and Volatile Solids

The organic fraction represents a substantial portion of biosolids and it is typically expressed as volatile solids (VS). Biosolids generally contain 40-60% VS on a total dry solids basis, comprising proteins, carbohydrates, lipids, humic substances, and microbial biomass (Fytili & Zabaniotou, 2008). The remaining fraction consists primarily of mineral ash, including oxides of calcium, magnesium, aluminum, iron, and silica, reflecting contributions from wastewater and treatment chemicals.

3.3.2 Macronutrients and Micronutrients

Biosolids are rich in several macronutrients essential for plant growth, including nitrogen (N), phosphorus (P), sulfur (S), calcium (Ca), and magnesium (Mg), which are largely incorporated within the organic matrix (Gilmour et al., 2003). They also contain variable concentrations of micronutrients such as manganese (Mn), copper (Cu), zinc (Zn), and molybdenum (Mo), contributing to their agronomic value (Gilmour et al., 2003). In contrast, potassium (K) concentrations in biosolids are generally low, and supplemental K fertilization may be necessary for sustained productivity in amended soils (Cogger et al., 2013).

Nutrient concentrations typically range from 1-11% total nitrogen and 0.7-7.5% total phosphorus on a dry-weight basis (O'Connor et al., 2005). Although these values are lower than those found in synthetic fertilizers-which commonly contain 15-82% N and 8-76% P the slow-release nature of biosolid-derived nutrients enhances their suitability as soil amendments (Price et al., 2015).

3.3.3 Trace Metals

The inorganic fraction of biosolids includes trace metals originating from household wastewater, urban runoff, industrial inputs, and corrosion of plumbing materials. Commonly detected metals include zinc (Zn), copper (Cu), chromium (Cr), nickel (Ni), lead (Pb), cadmium (Cd), and mercury (Hg) (Wuana et al., 2011). Although present at varying concentrations, these elements are strictly regulated under the U.S. EPA Part 503 Rule, which sets maximum allowable limits for land application to safeguard human health and environmental quality

3.3.4 Organic Micropollutants

Biosolids are also recognized as reservoirs for a range of organic contaminants that are only partially removed during wastewater treatment. These include:

- Pharmaceuticals and personal care products (PPCPs), such as antibiotics, analgesics, hormones, and antimicrobials (Walters et al., 2010; Clarke & Smith, 2011).
- Polycyclic aromatic hydrocarbons (PAHs), including phenanthrene, fluoranthene, and pyrene, which may originate from combustion sources and urban runoff (Inyang et al., 2016).
- Polychlorinated biphenyls (PCBs), typically present at low levels due to historical industrial usage (USEPA, 1999).

Many of these substances exhibit varying degrees of persistence, bioaccumulation potential, and ecological toxicity.

3.3.5 Microplastics

Wastewater treatment plants capture the majority (80-99%) of microplastics entering the system, resulting in their accumulation in the sludge and, consequently, in biosolids (Mahon et al., 2017). When biosolids are land-

applied, microplastics can persist in soils, where they may alter soil physical properties, interact with organic pollutants, or be transported through erosion processes (Corradini et al., 2019).

3.3.6 Per- and Polyfluoroalkyl Substances (PFAS)

PFAS have emerged as contaminants of particular concern in biosolids due to their strong chemical stability and resistance to degradation. These compounds are poorly removed during wastewater treatment and tend to partition into the solid phase.Frequently detected PFAS include perfluorooctane sulfonate (PFOS), perfluorooctanoic acid (PFOA), perfluorohexane sulfonate (PFHxS), perfluorobutane sulfonate (PFBS), and 6:2 fluorotelomer sulfonate (6:2 FTS) (Venkatesan & Halden, 2013; Lang et al., 2017; McDonough et al., 2022). Their persistence, mobility, and bioaccumulative potential raise concerns regarding their environmental fate following land application of biosolids.

3.4 Biosolids classification

Biosolids may be classified according to their stabilization characteristics and compositional properties, which influence their reactivity, nutrient availability, and suitability for agronomic use. From a functional standpoint, biosolids are often differentiated based on their nitrogen content, a key indicator of stabilization history and soil behavior. High-nitrogen (high-N) biosolids, typically containing 3-6% total nitrogen, undergo shorter stabilization periods and retain a high proportion of readily degradable organic matter. These materials tend to exhibit rapid microbial activity after land application due to the presence of short-chain organic compounds (Roman-Pérez et al., 2021; Gianico et al., 2021). Anaerobically digested, lime-stabilized, and heat-treated biosolids commonly fall within this category.

In contrast, low-nitrogen (low-N) biosolids, generally containing 1-3% total nitrogen, undergo longer stabilization often in lagoons or drying beds resulting in more stable organic matter and slower decomposition rates (Oun et al., 2014). While low-N materials may still function effectively as nutrient sources, higher application rates are typically required to meet crop nitrogen demands (Mohajerani & Karabatak, 2020). Their higher solids content and lower biological reactivity reflect extended natural drying and breakdown of easily degradable polymers or organic fractions.

3.5 Global Perspective

Globally, biosolids production is increasing in response to population growth, expanding wastewater treatment infrastructure, and stricter effluent quality regulations.

Currently, there is no consensus in the literature regarding the total global production of sewage sludge; it must be estimated from the most recently published statistical data. At the regional level, the annual cumulative production of dry sewage sludge in the 27 countries of the European Union is estimated at approximately 9.25 million tonnes (Feng et al., 2023). On a global scale, the worldwide production of biosolids is estimated to be around 100-125 million tonnes per year and is expected to continuously increase, reaching approximately 150-200 million tonnes by the end of 2025. This growth is primarily driven by population increase, urbanization, and the expansion of wastewater treatment infrastructure worldwide (Mohajerani et al., 2017).

At the national scale, production varies substantially. Canada generates approximately 660,000 dry tons per year (Canadian Council of Ministers of the Environment, 2012), while the United States produces around 13.84 million dry tons annually (Seiple et al., 2017). These increasing volumes highlight the importance of sustainable biosolids management strategies that address both agronomic potential and environmental risks, motivating interest in advanced treatment technologies.

3.6 US Regulatory Framework

Biosolids management is governed by national and regional regulations that define treatment requirements, quality standards, and permissible uses. In the United States, the principal legislation is the U.S. EPA Part 503 Rule, promulgated in 1993 and codified in 40 CFR Part 503, which establishes limits for pollutants, pathogen reduction criteria, vector attraction reduction, and monitoring requirements. The rule applies to all wastewater treatment facilities producing biosolids and has influenced similar frameworks internationally.

Under the Part 503 Rule, biosolids are classified into Class A or Class B based on pathogen reduction performance. Class A biosolids must meet strict process and microbiological standards that reduce pathogens to undetectable levels, enabling unrestricted use, including in residential settings. Class B biosolids undergo less intensive treatment and may contain detectable pathogens; therefore, their use is allowed only with specified site management restrictions to limit human and animal exposure. Class A biosolids are typically produced through processes such as composting, heat treatment, or pasteurization, while Class B materials are commonly generated through anaerobic digestion or lime stabilization.

The Part 503 Rule permits three primary management pathways: land application, surface disposal, and incineration, each accompanied by requirements to ensure environmental and public health protection. Land application is the most common route, supporting beneficial reuse, while surface disposal and incineration are used when land application is impractical or restricted.

3.7 European Regulations on Biosolids and Biochar

The European Union (EU) maintains strict guidelines on the land application of biosolids, primarily through the Sewage Sludge Directive (86/278/EEC), which limits concentrations of heavy metals and mandates safe agricultural reuse. However, specific regulation for PFAS in biosolids is still emerging. Recent EU actions include setting maximum permissible concentrations of PFAS in drinking water (EU Drinking Water Directive 2020/2184) and regulating PFAS as substances of very high concern (SVHC) under REACH.

For biochar, the European Biochar Certificate (EBC) sets quality standards, including thresholds for contaminants such as PAHs and heavy metals. Although PFAS are not yet fully regulated in this context, ongoing discussions indicate a potential future inclusion.

3.8 Canadian Guidelines and Provincial Practices

In Canada, biosolids are managed through a combination of federal guidance and provincial regulations. The Canadian Council of Ministers of the Environment (CCME) provides national guidelines promoting beneficial use of biosolids, while provinces such as British Columbia, Ontario, and Quebec enforce more detailed frameworks regarding contaminants and land application.

PFAS regulation in biosolids remains limited at the federal level, but provincial authorities are increasingly studying PFAS occurrence and management. For example, Ontario's MECP (Ministry of Environment, Conservation and Parks) is currently evaluating PFAS risks in land-applied biosolids.

3.9 Comparison of Regulatory Approaches

While both the EU and Canada promote the land application of biosolids under controlled conditions, the EU appears more proactive in regulating PFAS in drinking water and consumer goods. Canada's approach remains primarily risk-based and decentralized, with varying levels of enforcement among provinces. Both regions are converging toward stricter controls, and thermal treatments like pyrolysis could serve as a proactive solution to emerging PFAS regulations.

4 Contaminated PFAS Biosolids Treatment technologies

Figures 4.1-4.2 illustrate that, both in the United States and Europe, **land application remains the predominant pathway for biosolids management**, followed by landfilling and, to a lesser extent, incineration. These practices reflect long-standing strategies aimed at nutrient recycling and waste reduction. However, the widespread land application of biosolids is increasingly challenged by the presence of persistent contaminants such as PFAS, which **are not degraded by conventional stabilization processes**

Traditional treatment methods including coagulation, flocculation, and activated-carbon adsorption have proven insufficient for the complete removal or destruction of PFAS from wastewater and biosolids. This limitation has accelerated interest in more advanced technologies, such as electrochemical oxidation, plasma-based treatments, engineered biochars, carbon nanotubes, and graphene oxide, which offer higher adsorption capacities and can be tailored for PFAS selectivity (Srivastava et al., 2025).

Among these emerging solutions, **thermal conversion technologies particularly pyrolysis have gained significant attention**. Pyrolysis treats sewage sludge under oxygen-limited conditions at 350-650 °C (low temperature) or 650-800 °C (high temperature), producing three useful outputs: a carbon-rich solid (biochar), condensable vapors, and non-condensable gases. Several recent studies have demonstrated that pyrolysis at moderate temperatures (around 400 °C) can substantially reduce PFAS concentrations in sewage sludge (Hušek et al., 2024), although fluorinated byproducts may partition into volatilized or condensable fractions requiring additional downstream treatment.

Other thermal technologies, including incineration, gasification, and supercritical water oxidation (SCWO), also offer potential pathways for PFAS destruction. Incineration can achieve high destruction efficiencies but may generate halogenated byproducts if not properly controlled. Gasification (600-800 °C) enables partial mineralization yet may form intermediate toxic compounds, while SCWO can effectively oxidize PFAS at high pressure but remains economically challenging to implement at full scale (Srivastava et al., 2025).

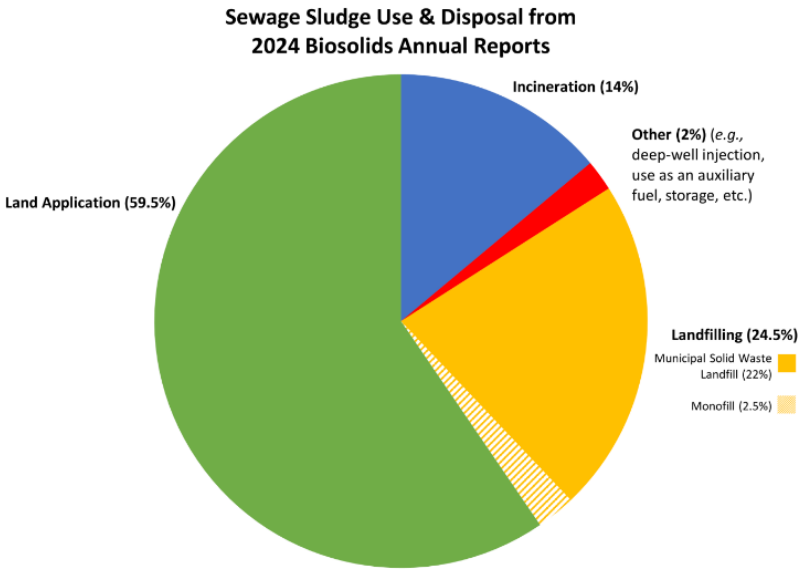

Figure 4.1: Distribution of sewage sludge use and disposal practices in the 2024 based on 2024 biosolids annual reports (U.S. EPA, 2024).

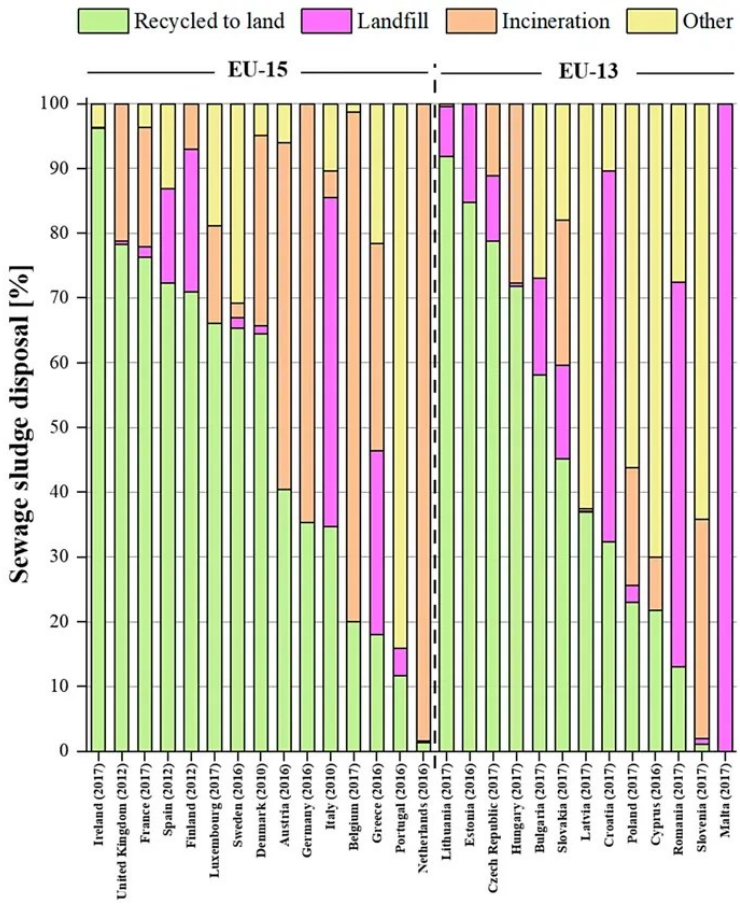

Figure 4.2: Sewage sludge disposal routes in the European Union; Source: Corradini et al., 2019 based on Eurostat 2018.

4.1 Fundamentals of Pyrolysis

Pyrolysis is a thermochemical process in which organic materials are decomposed at elevated temperatures typically between 300 and 800 °C in the absence of oxygen. In contrast to combustion or gasification, pyrolysis prevents oxidative reactions and promotes thermal cracking, yielding three primary product streams:

- Biochar, a carbon-rich solid residue;
- Bio-oil, composed of condensable organic vapors;
- Syngas, a mixture of non-condensable gases such as CO, CO_2, and CH_4 and light hydrocarbons

The relative yield of these products is influenced by feedstock characteristics as well as operational conditions, including temperature, residence time, heating rate, and reactor configuration

4.2 Pyrolysis Modes and Operating Parameters

Pyrolysis processes are typically classified according to heating rate and vapor residence time:

- Slow pyrolysis, characterized by low heating rates and long residence times, maximizes biochar production.
- Fast pyrolysis, employing rapid heating and short residence times, is designed to maximize bio-oil yield.
- Intermediate pyrolysis produces a more balanced distribution of char and liquids.

Key operational parameters include:

- Temperature, which strongly influences devolatilization, product yields, and PFAS degradation pathways;
- Residence time, affecting the extent of thermal conversion and secondary reactions;
- Sweeping gas flow (commonly nitrogen), used to maintain inert conditions and remove vapors from the reaction zone;
- Catalysts or additives, which may enhance PFAS degradation or promote fluorine immobilization within the char.

4.3 PFAS Degradation During Pyrolysis

Pyrolysis, operating between 300 and 700 °C in an oxygen-free environment, offers a promising pathway for PFAS degradation while minimizing greenhouse gas emissions and limiting the release of toxic metals. In addition to contaminant reduction, pyrolysis generates valuable end products such as biochar, bio-oil, and syngas, as discussed by Sivaram et al., (2022) and Wang et al., (2013). Because the process involves elevated temperatures, it is generally hypothesized that PFAS and other persistent organic contaminants in biosolids may undergo thermal decomposition, while carbon and nutrient contents can be retained in the resulting biochar, as emphasized by Longendyke et al., (2022) and Winchell et al., (2021).

Despite this potential, the literature on PFAS destruction during biosolids pyrolysis remains limited and often inconsistent. For example, Kim et al., (2015) reported no significant PFAS removal at 700 °C with a 3-hour solids residence time in a laboratory setup, whereas other studies including those by Bamdad et al., (2022) and Sørmo et al., (2023) observed removal efficiencies approaching 97-100% at 600-800 °C. Kundu et al., (2021) similarly found PFAS concentrations dropping below detection limits (<0.2 ng/g) in biochar produced at 500-600 °C in a semi-pilot-scale reactor. However, many studies do not report essential operational parameters, such as gas and solid residence times, resulting in uncertainty regarding the conditions required for reliable PFAS destruction.

Current understanding suggests that during pyrolysis, PFAS may primarily devolatilize rather than fully mineralize, meaning that volatilized PFAS or their intermediates may require further treatment. Consequently, complete destruction is often assumed to require the use of a secondary thermal oxidizer operating at temperatures >900 °C with residence times of at least 2 seconds, as indicated by Winchell et al., (2021); Zhang et al., (2023) and Meegoda et al., (2020). This requirement substantially increases capital and operational costs, posing challenges to the viability of commercial-scale pyrolysis systems for PFAS mitigation.

4.4 Additives key role

Catalytic pyrolysis has gained increasing attention as an approach to enhance PFAS degradation efficiency during thermal treatment. Several studies have demonstrated that specific additives particularly lime can substantially accelerate PFAS decomposition at low to moderate temperatures (<400 °C). Work by Sasi et al., (2021) as well as investigations by Wang and co-authors (2013, 2015), showed that these additives can promote earlier onset of PFAS breakdown compared with pyrolysis alone.

Among the various additives tested, lime ($Ca(OH)_2$) has repeatedly emerged as one of the most effective. Its role is twofold: it not only increases the pH and promotes thermal cracking, but more importantly, it captures fluorine released during PFAS decomposition, forming calcium fluoride (CaF_2) a thermodynamically stable and environmentally inert compound.

Despite these promising findings, the catalytic mechanisms involved in PFAS decomposition during pyrolysis and co-pyrolysis remain only partially understood. The influence of additive dosage, distribution within the matrix, reaction intermediates, and interactions with biosolid constituents still requires systematic investigation. As a result, the use of additives represents a promising but not yet fully optimized strategy for PFAS mitigation in thermal processes, highlighting the need for further research.

4.5 Overview of Reactor Types for Sludge Pyrolysis

Fixed-bed reactors represent the simplest design and are widely used for laboratory studies, although heat transfer limitations can affect performance with heterogeneous materials such as biosolids. Rotary kilns allow continuous operation and improved mixing, making them suitable for large-scale applications. Fluidized-bed reactors provide excellent temperature uniformity and reaction kinetics due to efficient gas-solid contact, but require careful control of feed properties. Continuous Stirred-Tank Reactors (CSTRs) offer uniform mixing and controlled residence times, making them particularly suitable for mechanistic investigations and parametric studies.

4.6 Design and Operation of the Experimental Reactor

The experimental apparatus consists of:

- **A vertically mounted cylindrical reactor** equipped with an internal mechanical stirrer;
- **Multiple thermocouples** for real-time temperature monitoring;
- **A continuous nitrogen flow** to maintain inert, oxygen-free conditions;
- **A condensation train** to separate liquids from vapour-phase products;
- **A gas collection system** for pyrolysis gas measurement and sampling.

Pyrolysis trials were conducted at 500 °C and 650 °C, with residence times of 15 and 30 minutes. For each condition, PFAS concentrations were quantified in the biochar and condensate fractions to evaluate removal efficiency and the distribution of PFAS-derived fluorine across the pyrolysis products. Gas composition was analyzed separately to characterize the non-condensable products.

5 Research Context and Objectives

5.1 Current Knowledge Gaps in Biosolids Pyrolysis

Although pyrolysis has been proposed as a promising approach for mitigating PFAS contamination in biosolids, several knowledge gaps remain. In particular, there is still a limited understanding of PFAS behavior during thermal treatment in complex matrices such as wastewater-derived biosolids. The partitioning of PFAS among solid, liquid, and gaseous products during pyrolysis is not yet well characterized, and reported results vary depending on reactor configuration and operating conditions. In addition, the lack of standardized experimental setups across studies makes it difficult to directly compare results from the literature. Finally, there is a growing need for treatment approaches that both reduce PFAS contamination and preserve the potential valorization of biosolids-derived products, such as nutrient-rich biochar.

These gaps highlight the importance of controlled experimental investigations performed under well-defined thermal conditions.

5.2 Focus and Scope of This Thesis

This thesis investigates the behavior of PFAS during biosolids pyrolysis under controlled experimental conditions. The study focuses on evaluating the influence of key operational parameters, including pyrolysis temperature (500 °C and 650 °C) and solid residence time (15 and 30 minutes). Additional experiments involving PFAS spiking and the addition of selected additives were conducted to explore their influence on PFAS partitioning and the redistribution of PFAS-derived fluorine during the pyrolysis process.

The main outcomes assessed in this work include:

- PFAS removal efficiencies from the solid phase;
- Product yield distribution among biochar, pyrolysis oil, and pyrolysis gas;
- Partitioning of measurable PFAS across product phases;
- The effect of additives on PFAS removal and fluorine retention in the char.

6 Matherials and Methods

6.1 Samples profiles

The biosolids cake used in this study was obtained through a solids-treatment pathway similar to that shown in Figure 3.1. Initially, **four different biosolids feedstocks** were collected and subjected to drying and grinding, followed by proximate analysis, in order to assess variability in moisture content, volatile matter, fixed carbon, and ash content.

Based on the results of the preliminary characterization, two feedstocks, designated as Feedstock A and Feedstock B (Figure 6.1), were selected for the experimental campaign, as they exhibited contrasting compositional properties, particularly with respect to ash content. This contrast was considered relevant for investigating the influence of feedstock composition on pyrolysis performance and PFAS behavior.

The selected samples were provided in individual sealed containers and are referred to throughout this thesis as Feedstock A and Feedstock B for confidentiality reasons. After drying and grinding, the processed material amounted to approximately 2.4 kg for Feedstock A and 3.0 kg for Feedstock B. These quantities represent the total mass of ground feedstock prepared and available for experimental work.

Only a fraction of each processed batch was used in the individual pyrolysis experiments, as each test required relatively small feedstock masses. All experiments were carried out using **one feedstock at a time**, and no mixing of different biosolids types was performed.

(a) (b)

Figure 6.1: Feedstock samples: (a) Feedstock A; (b) Feedstock B

6.2 Drying

The biosolid samples were air-dried at 90 °C using a laboratory oven (Figure 6.2). Drying time ranged from 3 to 13 hours depending on the initial moisture content of each feedstock.

Four biosolid feedstocks were initially dried and subjected to proximate analysis. Based on their moisture, volatile matter, and ash content, two samples were selected as representative feedstocks for the pyrolysis experiments.

Figure 6.2: Laboratory oven used for air-drying of biosolid samples

6.3 Grinding

The dried samples were then ground using motorized screwdriver of the pilote plant (Figure 6.3), and sieved to obtain a reduced particle-size fraction. Excessive grinding was avoided to minimize moisture and volatile loss due to heat generation and to reduce the formation of fines that could interfere with analysis.

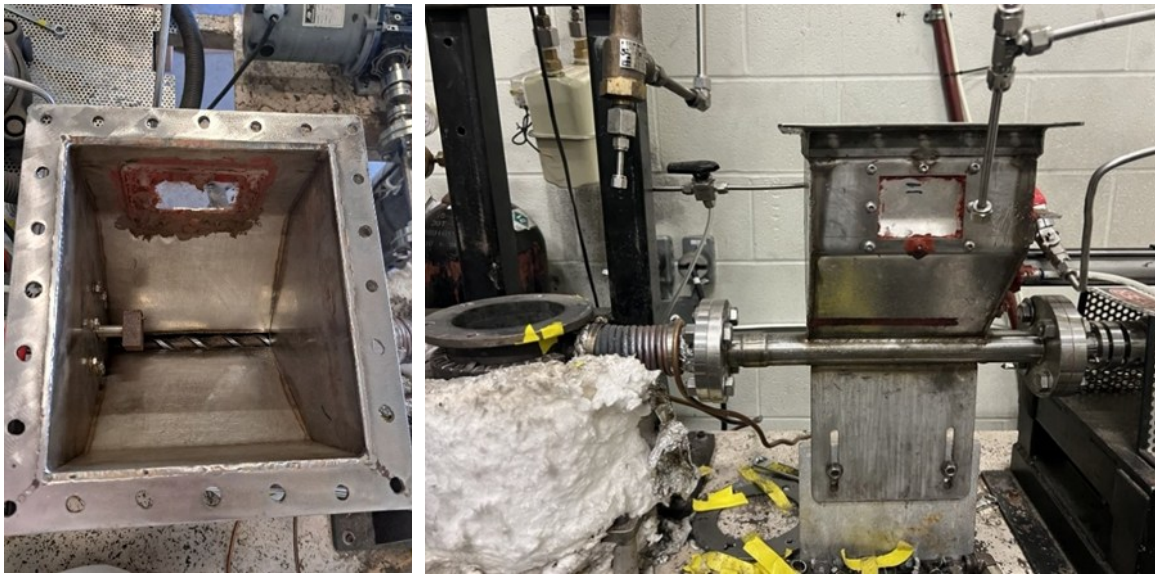

(a) (b)

Figure 6.3: (a) Internal configuration of the pilot-scale showing the screw-driven mechanism; (b) assembled grinding unit used to reduce the particle size of dried biosolid samples

6.4 Additive Preparation

Calcium hydroxide ($Ca(OH)_2$) in powder form was incorporated into the biosolid feedstock prior to the pyrolysis experiments. For each additive level, the required amount of $Ca(OH)_2$ corresponding to 5 wt% or 15 wt% of the dry biosolids was accurately weighed and placed in a ceramic mortar. The dried and ground

biosolid feedstock was subsequently added, and the mixture was manually homogenized using a spatula to ensure uniform distribution of the additive.

Following preparation, the $Ca(OH)_2$-biosolid mixtures were transferred to sealed and labeled containers and stored under dry conditions for several days prior to the pyrolysis trials. These containers served as pre-weighed feeding batches, enabling consistent reactor loading while preventing moisture uptake, contamination, or unintended reactions before processing.

6.5 PFAS Spiking Procedure

This section describes the procedure used to spike biosolid samples with selected PFAS compounds prior to the pyrolysis experiments. The objective of the spiking process was to introduce known quantities of PFAS into the biosolid matrix in order to evaluate their behavior during thermal treatment. The materials used, target concentrations, and detailed methodology applied for the spiking process are described in the following subsections.

6.5.1 Materials for spiking

PFAS spiking was performed using analytical-grade perfluorooctanoic acid (PFOA) and perfluorooctane sulfonate (PFOS) salts. HPLC-grade methanol (≥99.9% purity) was used as the solvent for preparing the spiking solutions. All solutions were prepared and handled in wide-mouth high-density polyethylene (HDPE) bottles to avoid PFAS adsorption onto glass surfaces.

6.5.2 Spiking loadings and target concentrations

The target PFAS concentration for the spiked biosolids was set at 2 mg of PFOA and 2 mg of PFOS per kg of dry biosolids. This loading was selected considering the background PFAS levels previously measured in the unspiked feedstocks (5-100 µg/kg for both PFOS and PFOA), ensuring quantifiable concentrations while remaining within realistic environmental ranges.

Based on preliminary trials and literature guidance on wet spiking methods for solid matrices, a ratio of 25 mL of methanol per 100 g of biosolids was adopted to ensure uniform PFAS dispersion. For the 300 g batches typically processed in this study, 75 mL of methanol-based spiking solution was used.

6.5.3 Spiking methodology

PFOS and PFOA salts were dissolved in 1.0-1.25 L of methanol inside a 1.5 L HDPE wide-mouth bottle to prepare a homogeneous spiking solution. The solution was placed on a benchtop shaker and agitated for 48 hours at 180 rpm to ensure complete dissolution.

Subsequently, 75 mL of the PFAS solution were added to 300 g of dried biosolids placed in a 1 L HDPE bottle. The mixture was shaken for 24 hours at 180 rpm to achieve uniform PFAS distribution throughout the biosolid matrix.

After shaking, the bottle was left uncapped in a fume hood for 24 hours to allow methanol evaporation. During this period, the material was manually stirred at intervals using a methanol-rinsed spatula to promote even drying and prevent agglomeration. The spiked biosolids were then sealed and stored at room temperature until use in the pyrolysis experiments.

7 Experimental Setup

The experimental setup used for the pyrolysis experiments is presented in Figure 7.1-7.2.

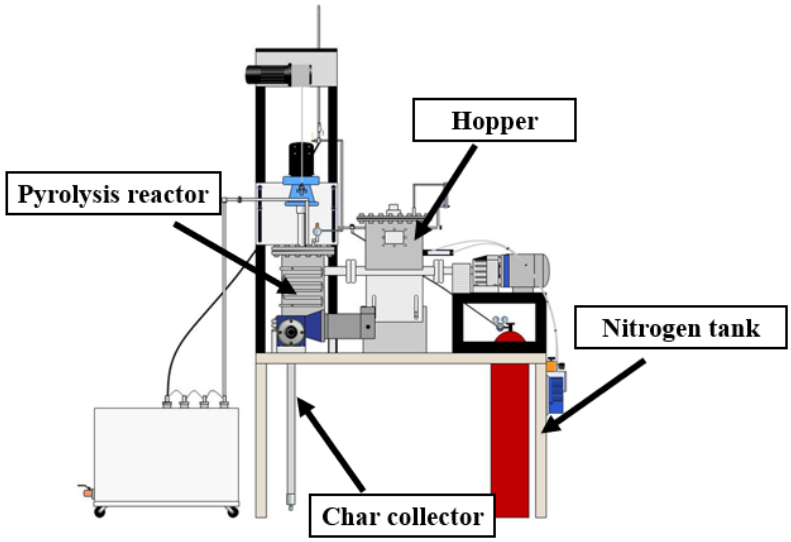

Figure 7.1: Schematic representation of the pyrolysis system used at the ICFAR facility (London, Ontario). The diagram illustrates the main operational units, including the feeding system, the pyrolysis reactor with mechanical agitation, the char extraction screw, and the multi-stage condensation and gas filtration train.

7.1 Feeding System

The biosolid feed was introduced into the reactor through a screw conveyor driven by an electric motor, which ensured a constant and controlled feeding rate. The motor speed was regulated via a dedicated control unit ("Feeding Motor") mounted on the right-hand panel.

To avoid material bridging inside the hopper, a mechanical bridge breaker was installed and operated through a separate control box equipped with an adjustable pressure valve.

A nitrogen flowmeter connected to an external N_2 line enabled system purging during startup and cooldown phases.

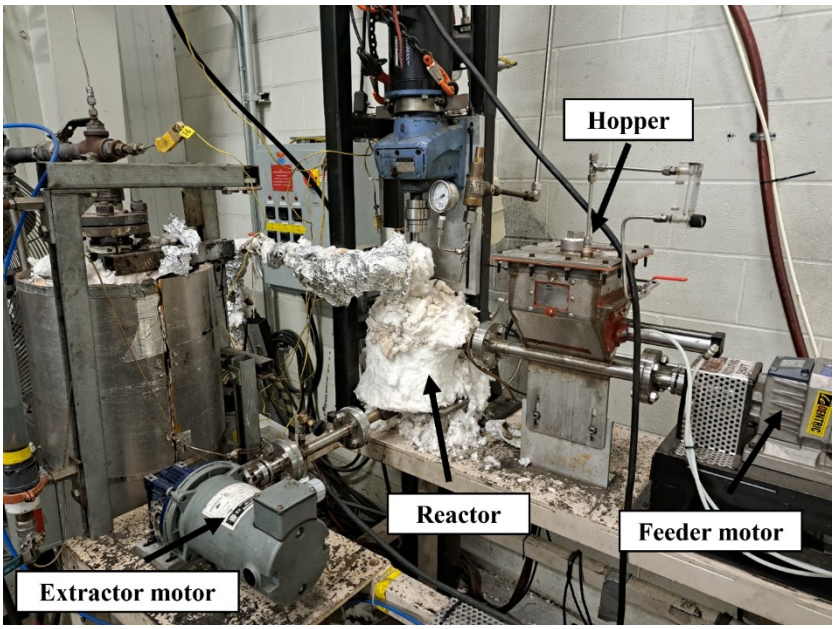

Figure 7.2: Photograph of the pyrolysis reactor system at ICFAR. From right to the right to the left image shows the actual configuration of the feeding unit, induction-heated reactor, insulation layers, gas handling line, during the experimental campaign**.**

7.2 Reactor Unit

The core of the setup consisted of a cylindrical pyrolysis reactor with internal dimensions of 18.4 cm in height and 13 cm in diameter (external dimensions: 23 × 16 cm). Heating was provided by an induction coil wrapped around the external wall, while thermal insulation minimized heat losses during operation.

Before steady operation was reached, a bed of char was formed inside the reactor. During continuous feeding, incoming biosolids were mixed with this hot char bed through a motorized agitator controlled by the "Agitating Motor" unit located on the main control panel. This configuration ensured effective mixing and promoted a uniform temperature distribution within the reactor.

Under steady-state conditions, the system behaves similarly to a continuously stirred reactor (CSTR) for the solid phase, while maintaining a char bed that provides thermal buffering and stabilizes the residence time of the solids.

Gaseous and vapor products exited the reactor through two lateral outlet lines equipped with fine mesh filters to prevent entrainment of solid particles. A third outlet located at the reactor top housed a pressure gauge for real-time pressure monitoring and incorporated a pressure relief valve together with an auxiliary exhaust line for emergency venting.

Reactor temperature was regulated using a dedicated control unit installed on the adjacent wall.

7.3 Char Extraction System

Solid char produced during pyrolysis was discharged through a motorized screw conveyor located at the base of the reactor. This system allowed either continuous or batch-mode extraction.

The extraction screw was operated via the "Extracting MTR" control unit placed on the right-hand panel, and the discharged char was collected in an external container.

7.4 Condensation and Gas Collection System

The vapor conditioning and gas collection system used in the experiments is illustred in Figure 7.3. Pyrolysis vapors passed through a five-stage vapor conditioning train consisting of three condensers followed by two filtration units. The first three units were cylindrical condensers arranged in series to progressively reduce the vapor temperature and promote condensation of the liquid fraction. Downstream of the condensers, the vapor stream entered two non-condensing filter units packed with alternating layers of cotton balls and silica, designed to remove fine particulates and residual aerosols before gas sampling.

The first four units (the three condensers and the first filter) were placed inside a water-cooled bath to enhance heat transfer efficiency, while the final filtration unit operated at ambient temperature.

In each stage, the vapor stream flowed from the inner tube toward the outer annular chamber (inner to outer flow configuration, improving thermal exchange, and uniform deposition of condensable species before exiting toward the next unit in the train.

Non-condensable gases were directed through the final exhaust line to a gas sampling system. A valve allowed the operator to switch the gas flow either toward a sampling bag for subsequent MicroGC analysis or directly to the exhaust.

At the terminal end of the line, a compressed-air-driven extractor provided the pressure differential needed to maintain continuous gas flow from the reactor through the entire system.

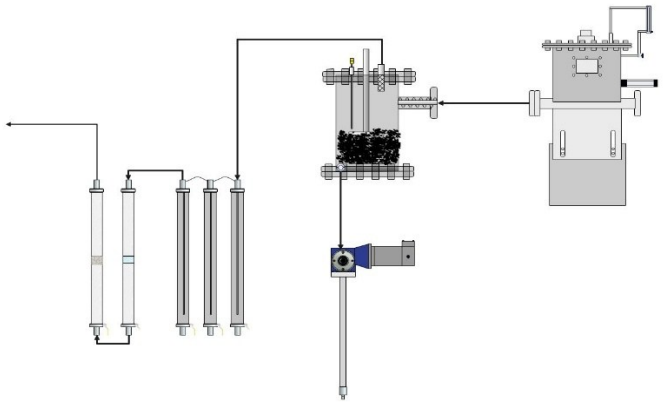

Figure 7.3: Schematic representation of the vapor conditioning and gas collection system used in the pyrolysis experiments, including the three condensers, two filtration units, and the gas sampling line.

7.5 Startup and Shutdown Procedures

Before each experimental run, the required amount of biosolid feedstock (with or without additive) was loaded into the hopper. Once filled, the hopper was sealed and fully closed to prevent air ingress during operation. Particular care was taken to ensure that all flanges, fittings, and connections along the reactor and gas-handling line were properly tightened.

Prior to heating, a pressure test was conducted for every experiment to verify system integrity. This procedure aimed to confirm the absence of pressure drops that could indicate leaks, as well as to identify any potential blockages or partially obstructed pathways within the reactor or downstream gas line. Only after confirming stable pressure behavior was the system considered ready for operation.

Before startup, both the reactor body and the entire gas line were carefully insulated to minimize heat losses and to ensure stable and uniform thermal conditions throughout the system. Nitrogen purging was then initiated to remove residual oxygen and establish an inert atmosphere within the reactor and vapor-handling train.

The reactor was subsequently heated to the target operating temperature under nitrogen flow, without feeding, until thermal stability was achieved. Once steady-state temperature conditions were reached, continuous feeding of the biosolids and activation of the char extraction system were initiated according to the defined operating parameters.

At the end of each run, the feeding system was stopped while nitrogen flow was maintained to prevent oxidation during the cooling phase. The reactor was allowed to cool under inert conditions before shutdown. After cooling, residual char was removed and the system was prepared for the subsequent experiment.

7.6 Operating Conditions

The target solids feeding rate for continuous operation was set at 5 $g \cdot min^{-1}$. Based on the calibration curve of the screw feeder, this corresponded to an operating frequency of approximately 3.2 Hz, which was used as the reference setting for all tests involving continuous feeding.

A target char extraction rate of 1.9 $g \cdot min^{-1}$ was defined, corresponding to an expected biochar yield of approximately 38%. However, calibration of the extraction screw revealed that the minimum achievable extractor frequency corresponded to a discharge rate of approximately 8 $g \cdot min^{-1}$. Achieving the desired extraction rate of 1.9 $g \cdot min^{-1}$ would therefore require a frequency below zero, which is physically impossible. This indicates that the minimum deliverable flow rate of the extraction system exceeded the design requirement, making direct continuous extraction at the target rate impractical.

To overcome this limitation, an on–off cycling strategy was implemented. The extraction screw was intermittently activated so that the time-averaged discharge rate approached the desired value of 1.9 $g \cdot min^{-1}$ while avoiding excessive removal of char during continuous operation.

Each pyrolysis experiment processed approximately 300 g of feedstock over a run time of one hour. Gas products were collected at 15, 30, and 45 minutes of operation to evaluate the temporal evolution of gas composition. For PFAS-spiked runs, gas sampling was not performed due to safety considerations associated with the potential release of fluorinated decomposition products under pyrolytic conditions.

7.7 Feeder and Extractor calibration

Calibration curves relating feeder motor frequency to solids mass flow rate were generated experimentally. A target feeding rate of 5 g/min corresponded to a frequency of 3.2 Hz.(Figure 7.4)

The extractor calibration revealed that the minimum achievable discharge rate was 8 g/min, significantly higher than the target value of 1.9 g/min.(Figure 7.5)

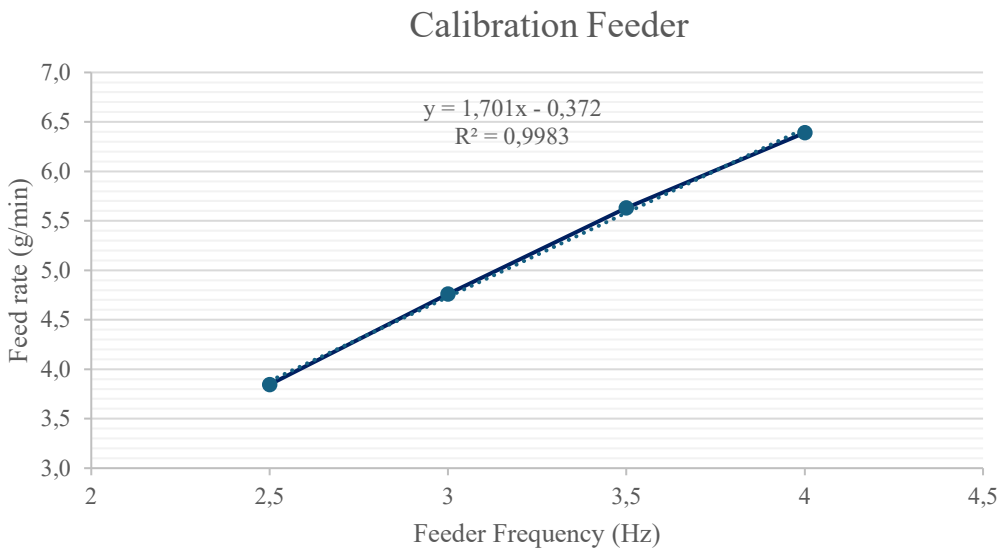

Figure 7.4: Calibration curve of the feeder, showing the relationship between feeder frequency and mass feed rate($g \cdot min^{-1}$),

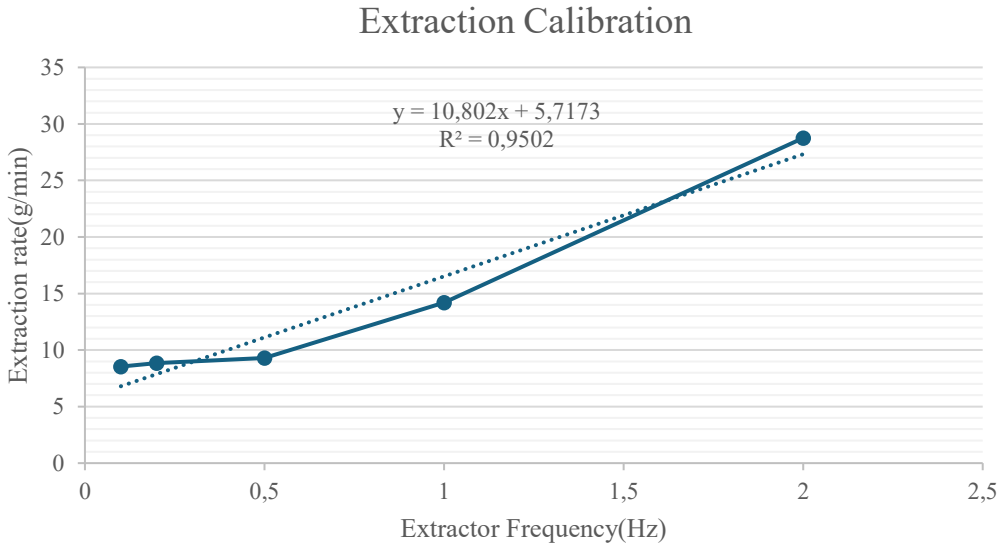

Figure 7.5: Calibration curve of the extraction system relating extractor frequency (Hz) to extraction rate ($g \cdot min^{-1}$)

7.8 Pyrolysis Parameters

- Temperature tested: **500 °C** and **650 °C**
- Residence time: **15** and **30 min**
- Sweep gas: 1l/min **N_2**
- Pressure 1 atm
- Heating mode: stable setpoint

7.9 Experimental Matrix

The feedstocks used in this work consisted of two municipal biosolids originating from different wastewater treatment plants. Pyrolysis experiments were conducted at 500 °C and 650 °C, with 15- and 30-minute solid residence times. For each temperature-residence time combination, at least three replicate runs were performed to ensure reproducibility. Additional repetitions were carried out when necessary to improve operational consistency and to verify the stability of the system under identical conditions.

During these tests, several maintenance actions were performed to ensure proper reactor sealing and stable operation, including the replacement of gaskets, installation of an additional inline filter, and substitution of worn bolts in the reactor flange assembly.

Subsequent tests evaluated the influence of calcium-based additive loading (5 wt% and 10 wt%) and PFAS spiking on product distribution and PFAS retention. Table 7.1 summarizes all the experimental conditions investigated in this study.

Table 7.1: Summary of experimental conditions for the pyrolysis tests

Date	Spiking	$Ca(OH)_2$	Run #	Temperature(°C)	RT(min)	Sample
1st May	N	N	1	500	15	Feedstock A
9th May	N	N	2	500	15	Feedstock A
12th May	N	N	3	650	15	Feedstock A
14th May	N	N	4	500	15	Feedstock A
15th May	N	N	5	500	15	Feedstock A
20th May	N	N	6	650	15	Feedstock A
22nd May	N	N	7	650	15	Feedstock A
29th May	N	N	8	500	30	Feedstock A
30th May	N	N	9	650	30	Feedstock A
2nd June	N	N	10	650	30	Feedstock A
5th June	N	N	11	500	15	Feedstock B
6th June	N	N	12	650	15	Feedstock B
11th June	N	N	13	650	30	Feedstock B
12th June	N	N	14	500	30	Feedstock B
17th June	N	N	15	500	30	Feedstock B
17th July	N	Y	16	500	15	Feedstock A
23rd July	Y	Y	17	500	15	Feedstock A
25th July	Y	Y	18	500	15	Feedstock A

7.10 Product Collection

During the pyrolysis experiments, the three product fractions (solid, liquid, and gas) were collected separately in order to quantify product yields and enable subsequent analyses. Solid char was recovered from the extraction system at the base of the reactor, while condensable vapors were collected as liquid products through the multi-stage condensation train. Non-condensable gases were sampled downstream of the vapor conditioning system using gas sampling bags for subsequent MicroGC analysis.

7.10.1 Solid Product (Char)

After system cooldown, the char collector located at the base of the reactor was disconnected and removed. The collected biochar was transferred inside a fume hood into pre-weighed containers and sealed to prevent moisture uptake.

A representative fraction of the char from each experiment was archived for PFAS analysis and additional characterization.

7.10.2 Liquid Product (Oil)

Condensable vapors produced during pyrolysis passed through a five-stage vapor conditioning train, consisting of three condensers followed by two non-condensing filtration units packed with alternating layers of cotton and silica. The first four units (three condensers + first filter) were immersed in a water-cooled bath to enhance heat transfer, while the last filtration unit operated at ambient temperature. Across all units, the vapor stream flowed from the inner tube toward the outer annular section, promoting efficient condensation and deposition of liquid products before exiting toward the downstream stage.

To quantify the liquid fraction, each condenser was weighed prior to each run. After the reactor was cooled to a safe handling temperature, the condensers were disconnected from the gas outlet line and removed from the cooling bath. Residual cooling water was expelled by gently blowing compressed air from the bottom port, ensuring accurate mass measurements. Inside a fume hood, the accumulated bio-oil was drained from each condenser into pre-weighed containers, sealed, and the condensers were subsequently re-weighed to determine residual adhered oil.

In addition to the condensate, the cotton layers from the first non-condensing filter were manually removed after each run and stored in pre-labeled containers. These materials were later used for PFAS analysis, as they retained PFAS-containing species not captured in the liquid fraction.

For each experiment, approximately a representative amount of bio-oil were transferred into labeled containers and stored at 4 °C for subsequent PFAS quantification.

7.10.3 Gas Products

Gas sampling was performed during each non-spiked pyrolysis run at 15, 30, and 45 minutes. Sampling was carried out by opening a dedicated valve located upstream of the exhaust line, allowing the gas stream to fill a pre-cleaned gas bag.

Before use, each gas bag was cleaned pro under a fume hood by repeated vacuum-purge cycles and kept sealed until sampling. Once filled, the bags were closed immediately analyzed in MicroGC or stored at 4°C temperature pending MicroGC analysis before 24 hours

Gas sampling was not performed during PFAS-spiked tests due to safety considerations related to potential fluorinated pyrolysis by-products.

8 Analytical Methods

8.1 Proximate Analysis

The proximate analysis, aimed at determining moisture, volatile matter, and ash content, was conducted following the standard ASTM D1762-84 (2013) method entitled *"Standard Test Method for Chemical Analysis of Wood Charcoal"*. This procedure is widely used for assessing the quality and composition of wood-derived charcoal, both in lump and briquetted forms.

In this work, the ASTM protocol was adopted with slight modifications in order to adapt the procedure to the available laboratory equipment and specific research needs.

According to ASTM D1762-84, the proximate analysis involves:

- **Moisture content**: determined by the weight loss after heating the sample at 105 °C for 2 hours.
- **Volatile matter**: measured by the weight loss after exposing the dried sample to 950 °C for a fixed time under specified conditions.
- **Ash content**: calculated from the remaining inorganic residue after combustion at 750 °C until constant weight.

8.1.1 Experimental Procedure

All analyses were performed in triplicate, and the results were averaged.

1. **Moisture determination**: Approximately 1.0 g of ground charcoal was weighed in a pre-dried porcelain crucible(750°C for 10 min) and placed in a ventilated oven at 105 ± 1 °C for 2 h. The crucibles were then cooled in a desiccator for 1h and reweighed.
2. **Volatile matter**: The oven-dried sample, in the same crucible with a lid, was introduced into a preheated muffle furnace at 950 ± 5 °C for 7 min.. After the heating period, the crucibles were cooled in a desiccator and weighed.
3. **Ash content**: The same crucible containing the residue was placed (uncovered) in a muffle furnace at 750 ± 5 °C for 6 h, or until the sample reached constant weight. The crucibles were then cooled and weighed.

8.1.2 Calculation

The proximate analysis results were calculated as follows:

$$Moisture\ (\%) = \frac{mass_{sample} - mass_{sample,105°C}}{mass_{sample}} . 100$$

$$Volatile\ matter\ (\%) = \frac{mass_{sample,105°C} - mass_{sample,950°C}}{mass_{sample,105°C}} . 100$$

$$Ash(\%) = \frac{mass_{residue}}{mass_{sample,105°C}} . 100$$

$$\text{Fixed Carbon}(\%) = 100 - \text{Moisture}(\%) - \text{Volatile matter}\ (\%) - \text{Ash}\ (\%)$$

The results of proximate analysis for the investigated biosolid feedstocks are reported in Table 8.1

Table 8.1: Proximate analysis of biosolids samples processed during pyrolysis experiments

Samples	Proximate Analysis(wt.%,dry basis)			
	M	**VM**	**A**	**FC**
Feedstock A	12,46	62,14	27,59	10,27
Feedstock B	6,67	58,64	31,65	9,71

All results are expressed on an as-received basis and reported to one decimal place. Replicates were considered acceptable when the difference between duplicates was within the tolerance limits stated in the ASTM standard (0.1% for moisture and ash, 0.5% for volatile matter)

8.2 Gas Analysis (MicroGC)

Gas samples collected in gas bags were analyzed using a Varian CP-4900 Micro Gas Chromatograph, a compact, multi-channel GC system designed for rapid on-line gas analysis

The MicroGC employs TCD detectors for all channels. As stated in the manual, TCD operation requires a stable reference gas; the system uses helium or argon as carrier gases, depending on the analytical requirement

Carrier gas pressure is regulated internally at 80 psi, ensuring reproducible flow through the micro-columns.

Gas from the sampling bag is drawn into the instrument using the built-in sampling loop, after which the injector rapidly switches and delivers a fixed gas volume into each column modules.

Analysis is fully automated, and each chromatographic run provides peak areas for all detectable species.

8.2.1 Instrument configuration

Gas samples were analyzed using a Varian CP-4900 Micro Gas Chromatograph. Each channel consists of a micro-GC module with its own injector, chromatographic column, thermal conductivity detector (TCD) and temperature control system.

In the configuration used in this study, the three channels were set up to cover complementary groups of species:

- Channel 1: permanent gases and lightest hydrocarbon. This channel was used for the separation and detection of H_2, O_2, N_2, CO and CH_4.
- Channel 2: CO_2 and C_2 hydrocarbons. This channel resolved CO_2, as well as the C_2 hydrocarbons C_2H_4 and C_2H_6.
- Channel 3: C_3-C_6 hydrocarbons. This channel was dedicated to the heavier light hydrocarbons, namely C_3H_6, C_3H_8, C_4H_{10}, C_5H_{12} and C_6H_{14}.

All channels operated isothermally and were equipped with TCD detectors. Helium and argon were used as carrier gases, with the column modules regulated at a pressure of approximately 80 psi, as recommended for the CP-4900 MicroGC. Gas samples from the bags were introduced via the built-in sampling loop and injector valve, which delivered a fixed gas volume simultaneously to all three channels, ensuring reproducible injection conditions.

8.2.2 MicroGC Calibration Procedure

Gas quantification was based on compound-specific calibration curves generated for each detectable species. Calibration was performed by analyzing certified gas standards containing known concentrations of the target compounds. For each channel, the MicroGC software recorded the peak area corresponding to each standard concentration, and a linear regression was used to obtain the calibration slope:

$$C = \text{slope} \times A$$

where C is the concentration and A is the measured chromatographic peak area.

Calibration curves were generated separately for each channel:

- Channel 1 (H_2, O_2, N_2, CO, CH_4)
- Channel 2 (CO_2, C_2H_4, C_2H_6)
- Channel 3 (C_3H_6, C_3H_8, C_4H_{10}, C_5H_{12}, C_6H_{14})

8.2.3 Gas Normalization

After calibration, the raw concentrations obtained from the three MicroGC channels were processed to derive the final gas compositions. Because pyrolysis was conducted under an inert nitrogen atmosphere and no oxygen was expected in the reactor, the MicroGC output was normalized by excluding O_2 and N_2 from the final composition.

Following this correction, the concentrations of all measured compounds were renormalized to a total of 100%, according to:

$$x_i^{\text{norm}} = \frac{x_i}{\sum x_i} \times 100$$

where $x_i$represents the calibrated concentration of species i excluding O_2 and N_2.

The resulting values were reported as molar percentages (mol%) This normalization procedure allows direct comparison among tests and eliminates the influence of inert carrier gases or artifacts introduced during sampling or analysis.

8.3 PFAS Analysis (LC-MS/MS)

PFAS were quantified using liquid chromatography coupled with tandem mass spectorometry. The analytical procedure followed EPA Method 1633 Rev.A, which provides standardized protocols for the determination of multiple compounds in enviromental matrices

8.3.1 Sample Preparation

All solid samples (biosolids and biochar) were shipped chilled and stored at 4 °C until analysis. Sample preparation followed EPA Method 1633 Rev. A. 0.5 g of biosolids and 5.0 g of biochar were weighed into 50 mL polypropylene centrifuge tubes. Isotopically labeled internal standards were added to each sample and allowed to equilibrate for 30 min at 1000 rpm.

Following equilibration, 10 mL of 0.3% ammonium hydroxide in methanol were added and the tubes were shaken for an additional 30 min at 1000 rpm. Samples were then centrifuged at 4000 rpm for 10 min, and the supernatant was transferred into a clean centrifuge tube.

Two additional extraction steps were performed by adding 15 mL and then 5 mL of 0.3% ammonium hydroxide in methanol, each followed by 30 min shaking and 10 min centrifugation at 4000 rpm. All extracts

(~30 mL total) were combined and evaporated under a gentle nitrogen stream at 55 °C to a final volume of 5-7.5 mL.

The concentrated extract was then diluted to 50 mL using Milli-Q water (18.2 MΩ·cm, <4 ppm). Samples were stored at 4 °C overnight before SPE cleanup.

8.3.2 Solid-Phase Extraction (SPE)

The following day, Bond Elut PFAS WAX cartridges (Agilent, USA) were prepared with silanized glass wool packed to mid-height of the cartridge barrel. Large-volume SPE reservoirs were attached to allow processing of the 50 mL extract.

Cartridges were cleaned in order with:

- 1% ammonium hydroxide in methanol
- Methanol

and conditioned with 0.3 M formic acid.

Extracts were loaded at 5 mL/min, followed by a wash with 5 mL of methanol:0.1% formic acid (1:1). PFAS were eluted with 5 mL of 1% ammonium hydroxide in methanol. A 1.5 mL aliquot of the eluate was transferred into polypropylene autosampler vials and stored at –20 °C until LC-MS/MS analysis.

8.3.3 Instrumental Analysis (LC-MS/MS)

Analyses were performed on an Agilent 1100 HPLC coupled to a SCIEX 6500 triple-quadrupole mass spectrometer operating in negative ESI.

Chromatographic separation was achieved on an Accucore® C18 column (100 × 3 mm, 2.6 µm) with a matching guard column. The mobile phases were:

- A: 2 mM ammonium acetate in 95:5 water:acetonitrile
- B: 2 mM ammonium acetate in 95:5 acetonitrile:water

The gradient (600 µL/min) was:

- 0–0.2 min: 100% A
- 0.2–8.8 min: linear increase to 100% B
- 8.8–17.8 min: hold at 100% B
- 17.8–22.8 min: re-equilibration to initial conditions

Instrument parameters for the monitored PFAS transitions (MRM) are summarized in Appendix A(Table A1)

8.4 Yield Calculations

Product yields were calculated based on the mass of condensed liquids, collected char, and the volume-normalized composition of the non-condensable gases.

8.4.1 Char yield

Char yield was determined as:

$$Y_{\text{char}}(\%) = \frac{m_{\text{char}}}{m_{\text{feedstock}}} \times 100$$

where m_{char} is the mass of biochar collected after cooling and $m_{\text{feedstock}}$ is the initial dry mass of feedstock.

8.4.2 Oil yield

The condensable liquid yield was calculated as:

$$Y_{\text{oil}}(\%) = \frac{m_{\text{oil}}}{m_{\text{feedstock}}} \times 100$$

where m_{oil} includes the mass of condensed liquid recovered from the three condensers and the mass retained inside the condenser walls (determined by pre- and post-run weighing).

8.4.3 Gas yield

Gas yield was derived by difference:

$$Y_{\text{gas}}(\%) = 100 - (Y_{\text{char}} + Y_{\text{oil}})$$

For selected runs, a gas-phase check using MicroGC composition and total gas volume was performed to confirm consistency with the mass balance.

8.5 PFAS removal efficiency

8.5.1 Concept and scope

Removal efficiency η quantifies the fraction of fluorine derived from PFAS molecules that is **not retained** in the solid char after thermal treatment. All comparisons are made on a **feedstock-normalized basis** (ng F per g of feedstock), which ensures comparability across tests with different yields or additive loads.

$$\eta = 1 - \frac{F_{\text{char}}}{F_{\text{feedstock}}}$$

where:

- $F_{\text{feedstock}}$: total fluorine in the dry feedstock (ng F · g^{-1} feed),
- F_{char}: total fluorine retained in the char, expressed per gram of feedstock (ng F · g^{-1} feed).

8.6 PFAS-to-fluorine conversion (F-factor)

PFAS concentrations are typically reported as mass of compound per mass of sample (ng PFAS · g^{-1}). To compute fluorine mass balances, each PFAS concentration is converted into its fluorine-equivalent value using:

$$F\text{-factor}_i = \frac{n_{F,i} \cdot M_F}{M_i}$$

where:

- $n_{F,i}$: number of fluorine atoms in molecule i,
- $M_F = 18.9984\,\text{g·mol}^{-1}$,
- M_i: molecular weight of PFAS species i.

8.7 Fluorine in oil and char: conversion and summation

After computing F-factors, the fluorine-equivalent concentration in a matrix (char,oil) is:

$$F = \sum_i (C_i \cdot F\text{-factor}_i)$$

where:

- C_i: concentration of PFAS species i in Dry Feedstock (ng PFAS · g^{-1} sample),
- F: fluorine-equivalent concentration (ng F · g^{-1} sample).

All PFAS contributions are summed.

8.8 Normalization to feedstock basis using char yields

With additives present (e.g., $Ca(OH)_2$), recovered char contains both biomass-derived material and additive residues. To compare fluorine retention per gram of original feedstock, char concentrations are normalized using:

Let:

- m_{feed}= dry mass of biosolids
- m_{add}= mass of additive in the feed
- $m_{\text{char,tot}}$= total solid mass recovered
- $m_{\text{char,org}} = m_{\text{char,tot}} - m_{\text{add}}$

Then:

$$Y = \frac{m_{\text{char,org}}}{m_{\text{feed}}}$$

The fluorine retained in the char on a feedstock basis is:

$$F_{\text{char}} = F_{\text{char,conc}} \cdot Y$$

where $F_{\text{char,conc}}$is the fluorine concentration measured in the char (ng F · g^{-1} char).

9 Results

9.1 Char, Oil, Gas Yields for All Conditions

Figures 9.1 and 9.2 show the char, oil and gas yields obtained under the different pyrolysis conditions tested (500 and 650 °C; 15 and 30 min), for both feedstocks (Feedstock A and Feedstock B),. Error bars represent the standard deviation of replicate runs..

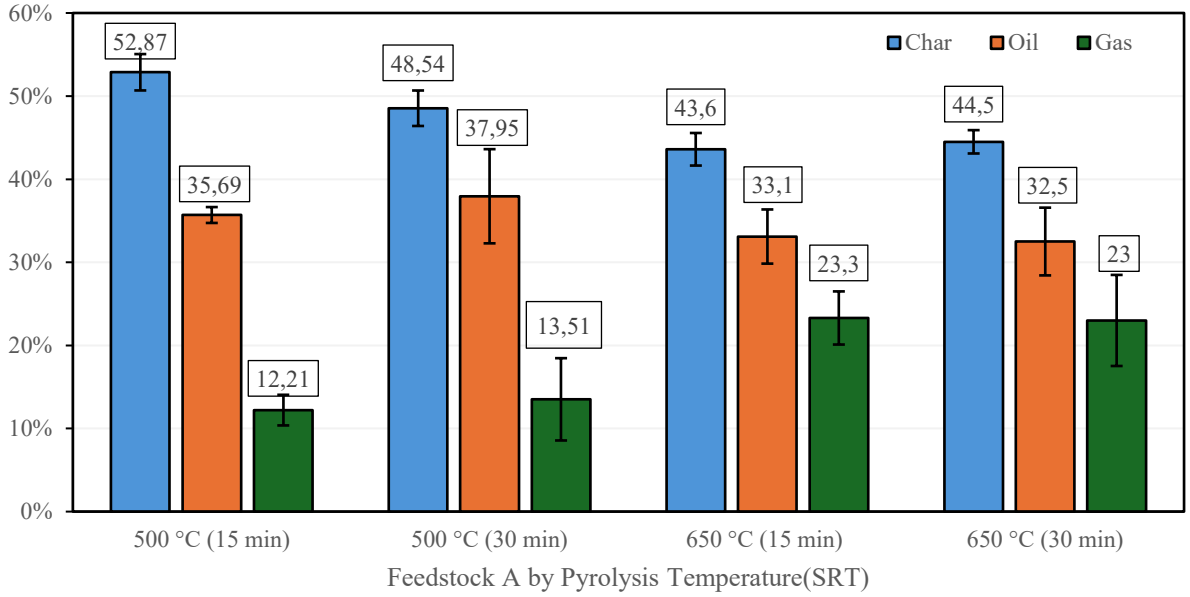

Figure 9.1: Char, oil and gas yields obtained from pyrolysis of the Feedstock A biosolid at different temperatures (500 and 650 °C) and solid residence times (15 and 30 min). Error bars represent the standard deviation of replicate runs.

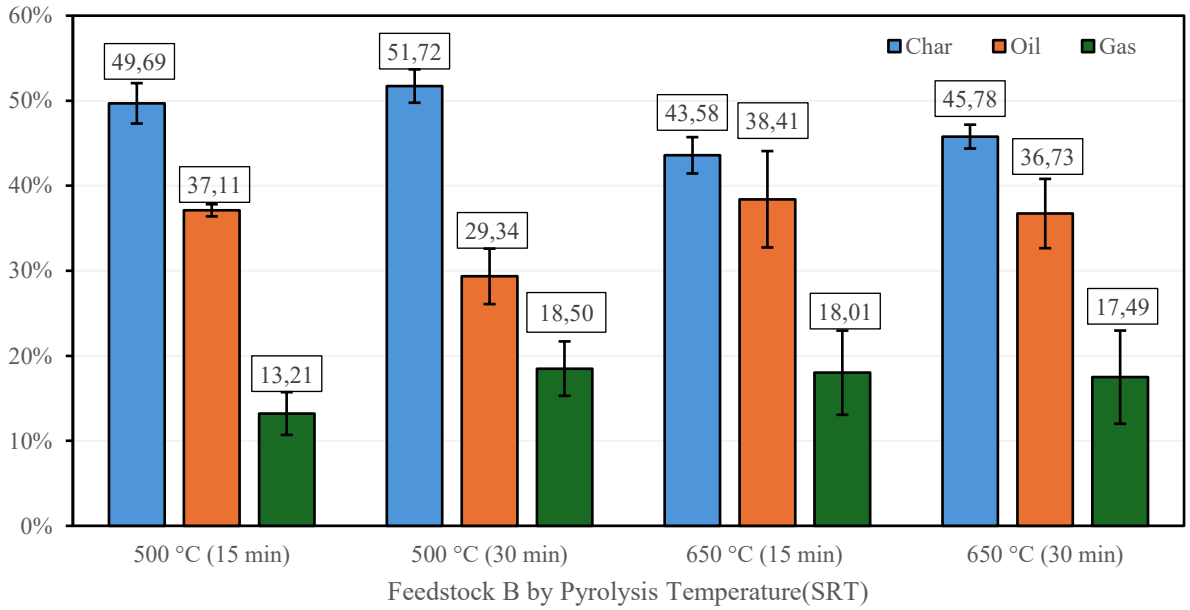

Figure 9.2. Char, oil and gas yields obtained from pyrolysis of the Feedstock B biosolid at different temperatures (500 and 650 °C) and solid residence times (15 and 30 min). Error bars represent the standard deviation of replicate runs.

9.1.1 Effect of temperature

Pyrolysis temperature was identified as the primary parameter controlling product yield distribution, in accordance with trends widely reported in the literature. Studies on sewage sludge and biosolids pyrolysis have consistently shown that increasing temperature leads to a progressive decrease in biochar yield and a corresponding increase in permanent gas production, while bio-oil yields tend to decrease at higher temperatures due to intensified secondary cracking reactions (Liu et al., 2017). This behavior reflects enhanced devolatilization of the organic matrix and thermal decomposition of condensable intermediates at elevated temperatures.

Consistent with these observations, increasing the temperature from 500 to 650 °C in the present study resulted in a systematic reduction in char yield for both Feedstock A and Feedstock B biosolids, accompanied by a pronounced increase in gas yield. Liquid yields exhibited comparatively smaller variations and showed a tendency to decrease at higher temperature, particulary for Feedstock A indicating the occurrence of secondary cracking reactions similar to those reported by Liu et al. (2017) and Rathnayake et al. (2025)**.** For Feedstock B, however, the trend was less evident and in some cases appeared to follow the opposite direction, which may be related to feedstock-specific composition.

These temperature-dependent trends are further supported by additional experiments conducted at the ICFAR facilities on the same feedstock and using the same experimental setup, in which a longer solid residence time (45 min) was applied. Under these conditions, increasing temperature similarly resulted in decreased char yields and enhanced gas production. The consistency of results obtained at ICFAR under different residence times reinforces the conclusion that pyrolysis temperature, rather than residence time, is the dominant factor governing product yield distribution.

9.1.2 Effect of residence time

Compared to pyrolysis temperature, the effect of solid residence time on product yield distribution was secondary and mainly associated with the extent of secondary reactions. Previous studies have reported that longer residence times promote further conversion of the raw material and favor the formation of gaseous products during pyrolysis (Malins et al., 2015), while the influence on char yield becomes negligible once residence time exceeds a certain threshold (N.Gao et al., 2017).

In the present study, increasing the solid residence time from 15 to 30 min resulted in higher gas yields at 500 °C for both biosolids, confirming that extended residence time enhances secondary cracking reactions. Changes in char and liquid yields were comparatively modest and feedstock-dependent. At 650 °C, product yields showed only minor variations between 15 and 30 min, indicating that the system approached a steady state in terms of solid conversion. This behavior is consistent with previous findings reporting limited sensitivity of char yield to residence time beyond approximately 20-25 min (N.Gao et al., 2017).

Overall, these results confirm that solid residence time influences product yields primarily through secondary reactions, while its effect remains subordinate to that of pyrolysis temperature.

9.2 Additive and spiked tests

As shown in Figure 9.3, the addition of calcium hydroxide significantly increased the char yield, as expected due to the contribution of the inorganic additive and the enhanced stabilization of carbonaceous material. At 500 °C and 15 min, char yields increased from 52% (no additive) to 51-57% depending on $Ca(OH)_2$ loading.

Gas yields were lower in the presence of calcium, ranging from 7-13%, reflecting reduced volatilization. Oil yields remained relatively stable (35-36%) and showed no measurable differences between additive-only and additive + spiking tests.

Importantly, PFAS spiking did not modify the overall mass distribution among char, oil and gas, indicating that the added PFAS mass was too small to influence bulk pyrolysis behaviour**.**

Overall, yields were primarily governed by temperature, followed by residence time and feedstock type. Calcium-based additives increased char formation and reduced gas production, but did not alter the qualitative trends observed across operating conditions.

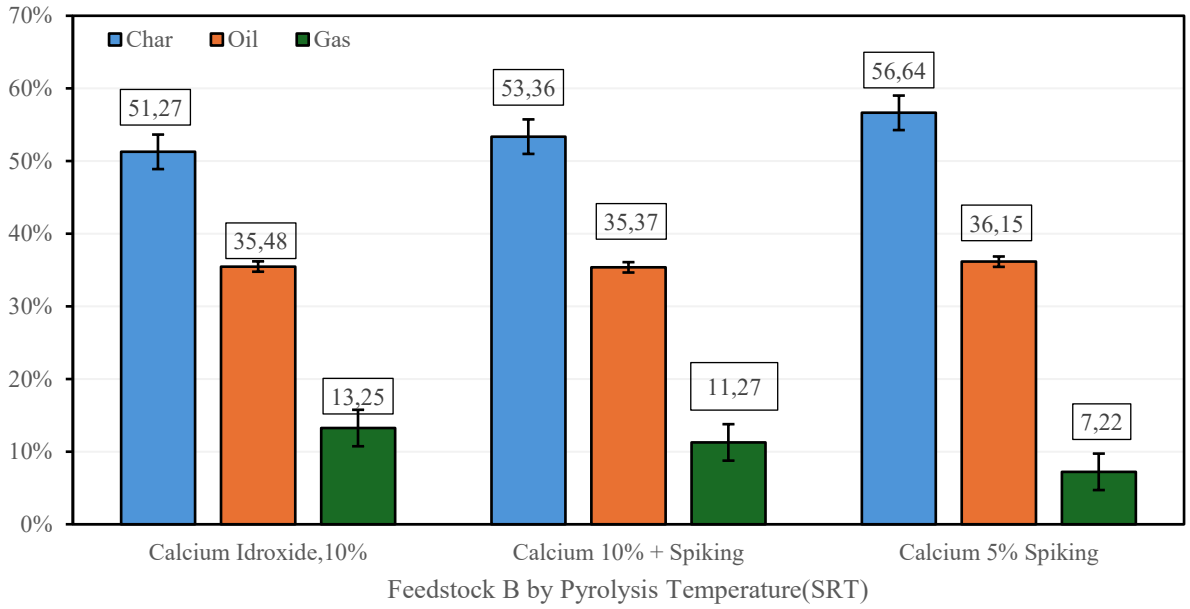

Figure 9.3: Effect of calcium hydroxide addition and spiking on product yield distribution (char, oil and gas) during pyrolysis of the Feedstock B biosolid at 500 °C RT:15 min.

9.3 Gas Composition from MicroGC

This section presents the gas compositions obtained from MicroGC analysis under the different pyrolysis conditions investigated (500 and 650 °C; residence times of 15 and 30 min). For each operating condition, gas samples were collected directly from the reactor at 15, 30 and 45 minutes during the run. These sampling times refer solely to the moment of gas withdrawal and do not represent different process conditions.

The objective of this section is to compare gas composition primarily as a function of temperature at fixed residence time (500 vs 650 °C at RT = 15 min, and again at RT = 30 min), while also illustrating the minor temporal variations observed within each run.

Figures 9.4 and 9.5 report the gas compositions obtained at 500 °C and 650 °C for a residence time of 15 min. For both conditions, gas samples were collected at 15, 30 and 45 min during the run; these sampling times only indicate when the gas was withdrawn and do not correspond to different process conditions.

At 500 °C (Figure 9.4), the gas was strongly dominated by CO_2 (≈73-75%), with relatively low amounts of CO (≈9-10%), CH_4 (≈5%) and very minor fractions of H_2 and C_2-C_3 hydrocarbons. The three sampling times yielded very similar compositions, indicating limited gas-phase evolution at this temperature.

At 650 °C (Figure 9.5), the gas composition changed markedly. CO_2 decreased to about 35-37%, while H_2 and CO increased substantially, and light olefins such as C_2H_4 and C_3H_6 became more abundant. This shift from a CO_2-rich to a more reduced gas mixture highlights the strong influence of temperature at constant residence time that it is also reported by Liu et al 2017, with higher severity promoting cracking reactions.

The same comparison at a residence time of 30 min is shown in Figures 9.6 and 9.7. At 500 °C (Figure 9.7), CO_2 again accounted for roughly 68-70% of the gas, with CO and CH_4 in the range of 8-11% and only minor H_2 and light hydrocarbons. As for RT = 15 min, the compositions at 15, 30 and 45 min were very similar, confirming that the gas profile is almost time-invariant at this lower temperature.

At 650 °C and RT = 30 min (Figure 9.6), the gas became even more reduced, with higher fractions of H_2, CO and C_2-C_3 hydrocarbons and CO_2 around 26-28%. Time-resolved sampling showed only modest changes during the run (slight increase in H_2, small variations in CH_4 and olefins), but the dominant effect remained the increase in temperature from 500 to 650 °C.

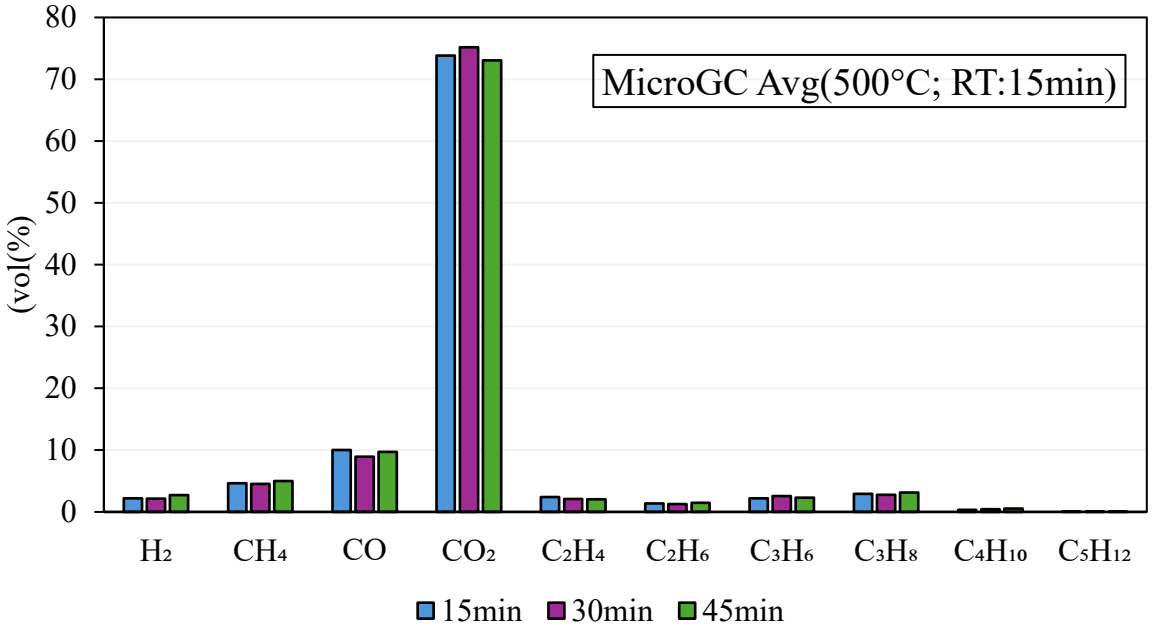

Figure 9.4. Average gas-phase composition measured by MicroGC during pyrolysis at 500 °C, RT:15 min based on gas samples collected at different times (15, 30 and 45 min) during the same experimental run

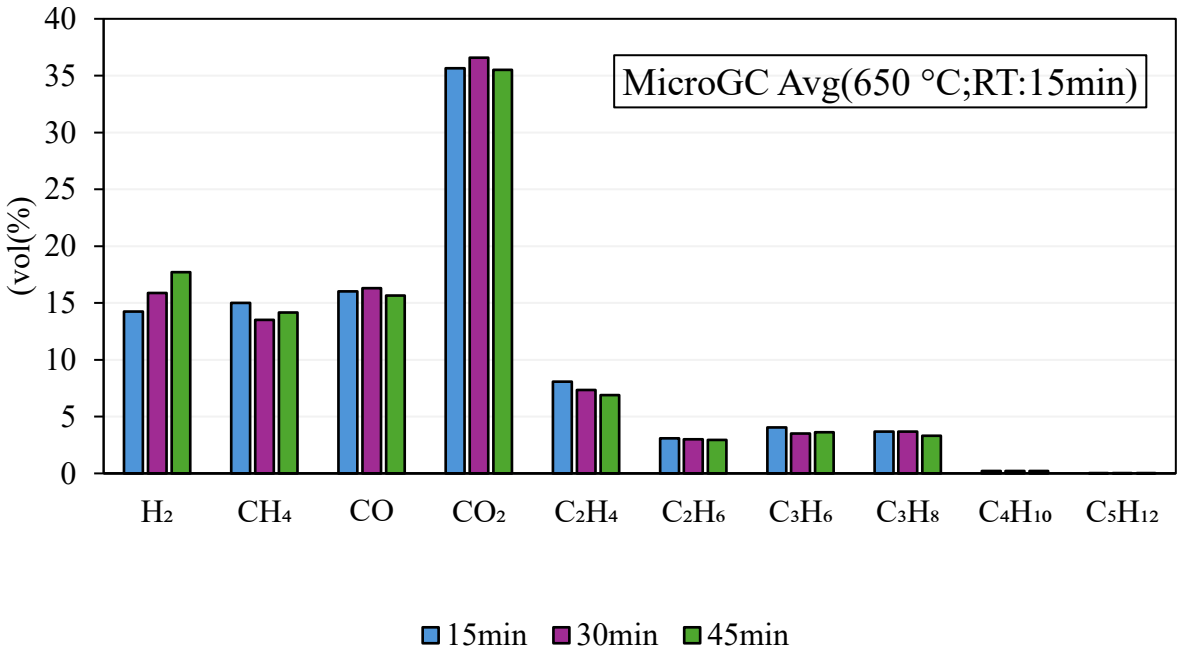

Figure 9.5. Average gas-phase composition measured by MicroGC during pyrolysis at 650 °C, RT:15 min based on gas samples collected at different times (15, 30 and 45 min) during the same experimental run

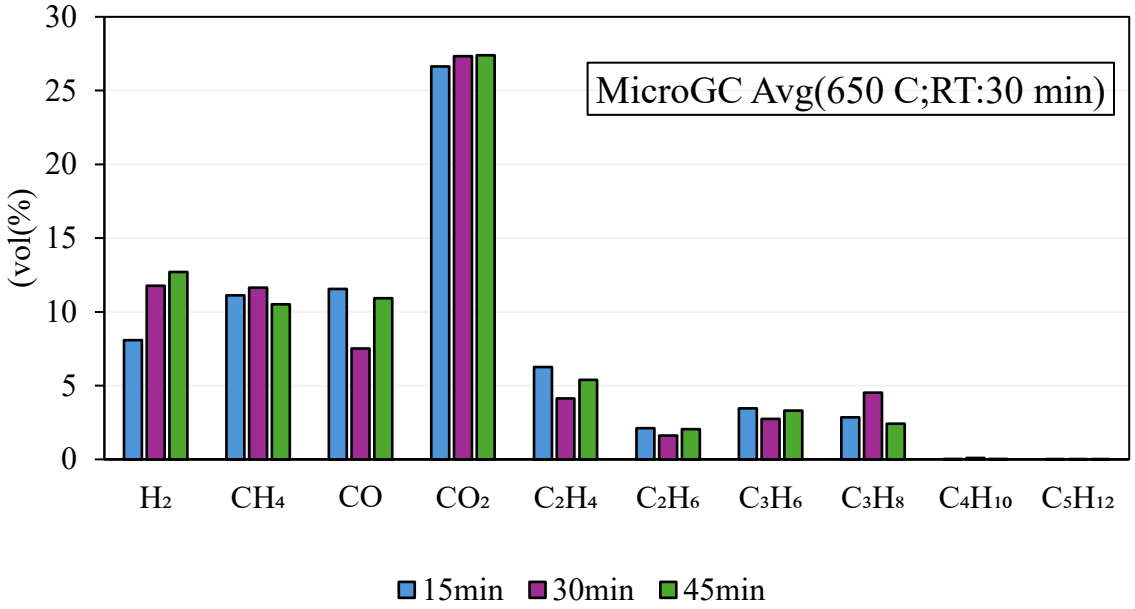

Figure 9.6. Average gas-phase composition measured by MicroGC during pyrolysis at 650 °C, RT:30 min based on gas samples collected at different times (15, 30 and 45 min) during the same experimental run

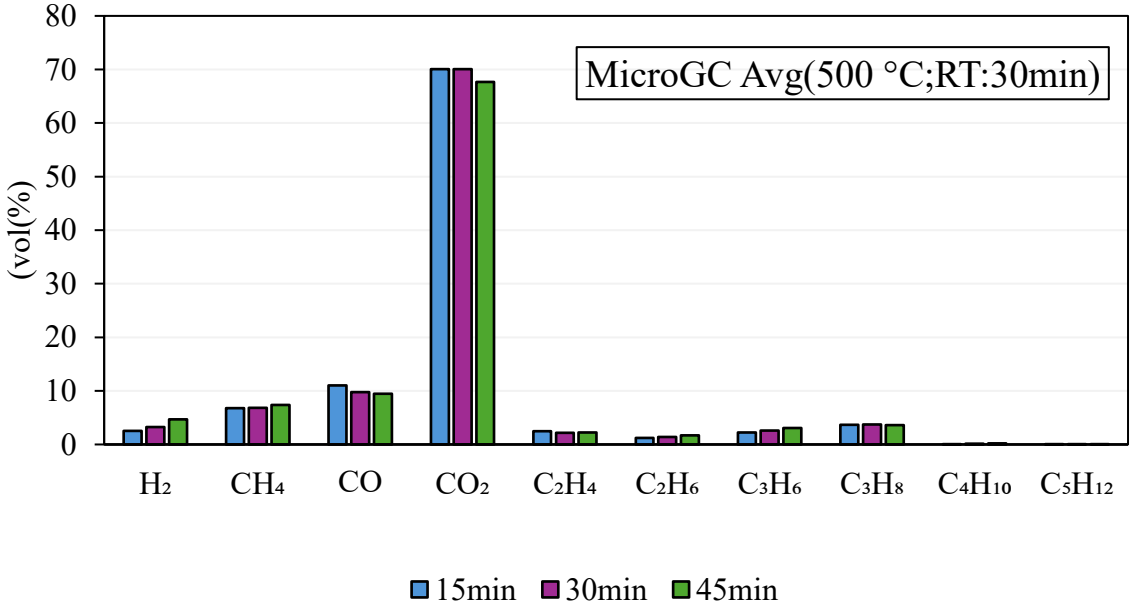

Figure 9.7. Average gas-phase composition measured by MicroGC during pyrolysis at 500°C, RT:30 min based on gas samples collected at different times (15, 30 and 45 min) during the same experimental run

9.4 PFAS Concentrations (Feedstock vs Char)

This section reports the PFAS concentrations measured in the feedstock and in the corresponding char samples obtained under the different pyrolysis conditions. PFAS data are presented both as individual compound concentrations (ng·g^{-1}) and as fluorine-equivalent concentrations (ng F·g^{-1}), obtained through the conversion factors described in methodology section. The objective is to quantify how much PFAS-derived fluorine

remains in the solid phase after pyrolysis and to compare retention levels across temperature, residence time and additive usage.

Two groups of experiments are included: (i) non-spiked tests, where PFAS are those naturally present in the biosolids; (ii) spiked tests, where controlled additions of PFOS and PFOA were performed to evaluate removal efficiency under known initial loads. A comparison with non-spiked char is also presented to determine the natural background contribution.

9.5 PFAS Concentrations in Non-Spiked Feedstock

The PFAS profile of the dry feedstock represents the reference point for all subsequent mass-balance and removal-efficiency calculations. A total of 23 PFAS species were detected in the Feedstock A biosolids, including perfluoroalkyl carboxylic acids (PFCAs), perfluoroalkyl sulfonic acids (PFSAs) and several precursor-type compounds. Table 9.1-9.3 reports their concentrations, grouped by chemical class and expressed on a dry-weight basis ($ng \cdot g^{-1}$). These values correspond to the analytical inputs used to compute fluorine-equivalent loads according to the methodology section.

As shown, the feedstock contains a complex mixture of legacy PFAS (e.g., PFOS, PFOA), long-chain PFCAs, and multiple precursor molecules such as FTCA, FTUCA and di PAP. Precursor-type PFAS dominate the overall burden, with 8:2 FTUCA representing the single largest contributor. These concentrations define the initial PFAS inventory against which the char-phase concentrations and removal efficiencies will be evaluated in the following section

Table 9.1 - Concentrations of perfluoroalkyl sulfonic acids (PFAS) detected in the dry biosolids feedstock (Feedstock A), expressed on a dry-weight basis ($ng\ g^{-1}$).

PFAS	Conc. Dry Feedstock(ng/g)
PFBA	4,52
PFHxA	14,74
PFHpA	6,08
PFOA	96,09
PFDA	14,5
PFUnA	2,04
PFDoA	5,71
PFTrDA	0,51
PFTeDA	0,98
PFHxDA	0,56
PFODA	377,77

Table 9.2 - Concentrations of perfluoroalkyl sulfonic acids (PFSAs) detected in the dry biosolids feedstock (Feedstock A), expressed on a dry-weight basis (ng g^{-1}).

PFSAs	Conc. Dry feedstock(ng/g)
PFBS	4,2
PFHxS	1,66
PFOS	47,05

Table 9.3 - Concentrations of PFAS precursor compounds detected in the dry biosolids feedstock (Feedstock A), expressed on a dry-weight basis (ng g^{-1}).

PFAS Precursors	Conc. Dry feedstock(ng/g)
6:2 FTS	16,68
8:2 FTS	1,78
8:2 diPAP	92,07
NMeFOSAA	26,29
NEtFOSAA	19,13
PFOSA	0,95
5:3 FTCA	78,48
8:2 FTUCA	3594,59
7:3 FTCA	66,23

9.6 Effect of Drying on PFAS Concentrations

A comparison between PFAS concentrations measured in wet and dry samples of Feedstock A (Figure 9.8) highlights notable differences in the distribution of several compounds. In particular, some PFAS species exhibit higher concentrations in the wet sample. This observation suggests that the drying step does not simply concentrate PFAS through water removal. Instead, certain compounds, especially precursor-type species such as 7:3 FTCA, 8:2 FTUCA, and 8:2 diPAP may partially volatilize, transform, or redistribute within the biosolids matrix during the drying step. Consequently, concentrations expressed on a dry-weight basis can appear lower than those measured in the wet sample. For consistency and comparability across experiments,

all PFAS mass-balance and removal-efficiency calculations presented in this thesis are therefore based on dry-weight concentrations.

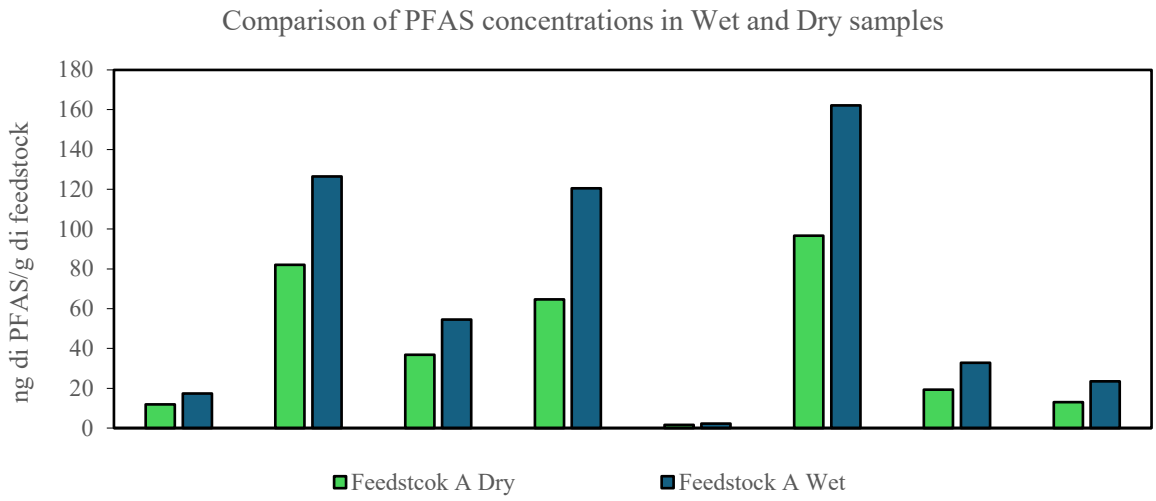

Figure 9.8. PFAS concentrations in the Feedstock A measured before and after drying, reported on a feedstock mass basis

9.7 Removal Efficiency

The removal efficiency of PFAS-derived fluorine under non-spiked conditions is presented in Figure 9.9. The results show a clear increase in efficiency with temperature, rising from approximately 95% at 500 °C to 97% at 650 °C, indicating reduced fluorine retention in the solid phase at higher pyrolysis temperatures. The presence of $Ca(OH)_2$ further improves removal efficiency, reaching values close to 99%. This behaviour is consistent with the formation of stable inorganic fluorides, such as CaF_2, which limit the incorporation of fluorine into the char matrix. Overall, these results suggest that both higher thermal severity and additive-assisted reactions contribute to minimizing the amount of fluorine remaining in the final solid product.

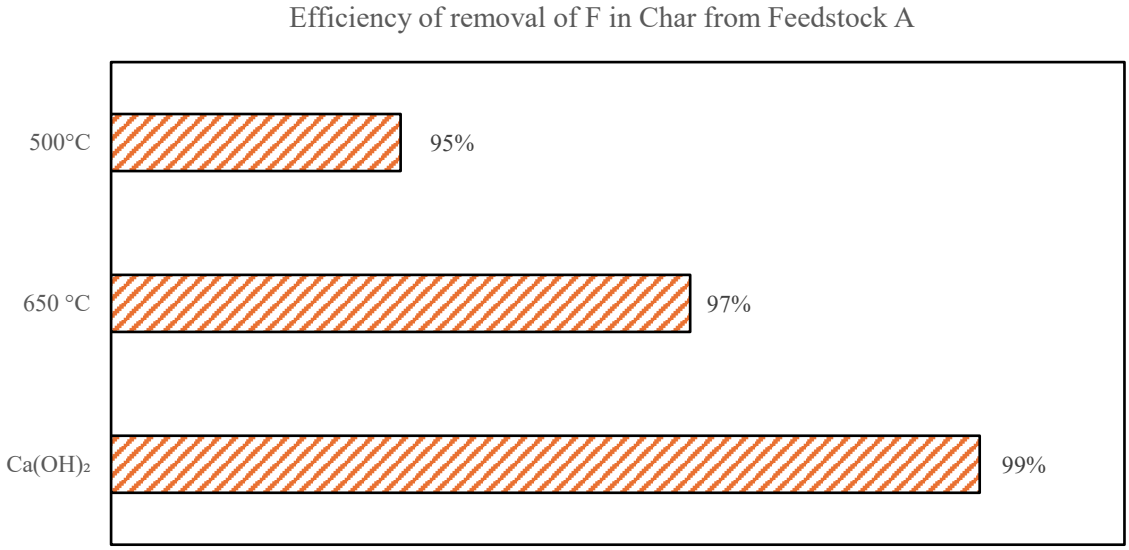

Figura 9.9: Efficiency of fluorine (F) removal from the biosolid feedstock into the char fraction under different pyrolysis conditions (500 °C, 650 °C) and with $Ca(OH)_2$ addition

This section reports the PFAS removal efficiency for all non-spiked tests, expressed as the fraction of fluorine not retained in the char. Across all operating conditions, pyrolysis resulted in high removal efficiencies, with values increasing with temperature. At 500 °C, the average removal efficiency was approximately 95%, while at 650 °C it increased to around 97%. These results indicate that increasing thermal severity enhances PFAS decomposition and limits fluorine retention within the solid phase.

The observed trend is consistent with previous findings reported in the literature. In particular, Rathnayake et al. (2025) demonstrated PFAS removal efficiencies exceeding 99% during biosolids pyrolysis when mineral additives were employed, highlighting the combined effect of elevated temperature and additive-induced reactions in promoting PFAS destruction and fluorine redistribution away from the solid phase. Although no additives were used in the present non-spiked tests, the high removal efficiencies achieved confirm the intrinsic effectiveness of pyrolysis in reducing PFAS retention in char, with temperature acting as a key controlling parameter

9.8 Efficiency for Spiked Tests

Spiked tests were performed only for PFOS and PFOA. The corresponding removal efficiencies were calculated using the theoretical fluorine load in the spiked feedstock and the measured fluorine remaining in the char.

In all cases, removal efficiencies were extremely high, typically ≥ 99%. Occasionally, F-char values were lower than the natural background measured in non-spiked chars, resulting in $\eta = 100\%$ (numerically 0 ng F/g retained). This effect reflects analytical uncertainty and the fact that the background fluorine is comparable to or larger than the residual spiked fluorine at these high removal levels.

9.9 Effect on PFAS Retention / Removal

The addition of $Ca(OH)_2$ had a measurable impact on PFAS behavior during pyrolysis. When calcium hydroxide was added to the feedstock, the fluorine retained in the char decreased further compared to non-spiked, non-additive tests. Removal efficiency reached values close to 99%, consistent with the formation of thermodynamically stable inorganic fluorides such as CaF_2, which reduce the amount of fluorine incorporated into the carbonaceous matrix.

These results suggest that $Ca(OH)_2$ not only enhances PFAS degradation but also immobilizes fluorine in mineral form, thereby improving the quality of the resulting char.

9.9.1 Spiking Experiments

Spiking experiments were conducted to evaluate PFOS and PFOA degradation under controlled and known initial PFAS loads.,A known concentration (2 mg/kg per compound) was added to the biosolids, ensuring that the PFAS concentration was sufficiently above natural background levels to allow robust quantification of removal.

Measured char concentrations were compared with both the theoretical spiked load and the background levels observed in non-spiked chars. In all spiking tests, residual PFOS and PFOA in char were extremely low, yielding removal efficiencies close to 99-100%. These results confirm that pyrolysis at the tested conditions is highly effective in decomposing both native and artificially enriched PFAS.

9.10 Distribution of PFAS-derived fluorine

To further evaluate the fate of PFAS during pyrolysis, the distribution of measurable PFAS-derived fluorine across the pyrolysis products was estimated based on the quantified PFAS concentrations in char and oil together with the corresponding product yields. Figure 9.10 illustrates the distribution of fluorine associated with targeted PFAS across the char, oil, and the fraction not recovered in the targeted PFAS analysis for two representative operating conditions: 500 °C and 650 °C at a residence time of 15 minutes.

At 500 °C, a relatively larger fraction of measurable PFAS-derived fluorine was detected in the oil fraction, indicating that part of the fluorinated compounds remained associated with condensable products under these thermal conditions. In contrast, the fraction of fluorine retained in the char remained comparatively small.

When the pyrolysis temperature was increased to 650 °C, the amount of measurable PFAS-derived fluorine detected in the oil fraction decreased significantly. At the same time, a larger portion of fluorine was not recovered in the targeted PFAS analysis. This trend suggests that increasing the temperature promotes the transformation of PFAS into volatile or non-target fluorinated species that are not captured within the analyzed PFAS compounds.

Overall, the results indicate that higher pyrolysis temperatures favor the redistribution of PFAS-derived fluorine away from condensable products and toward fractions that are not recovered in the targeted PFAS analysis.

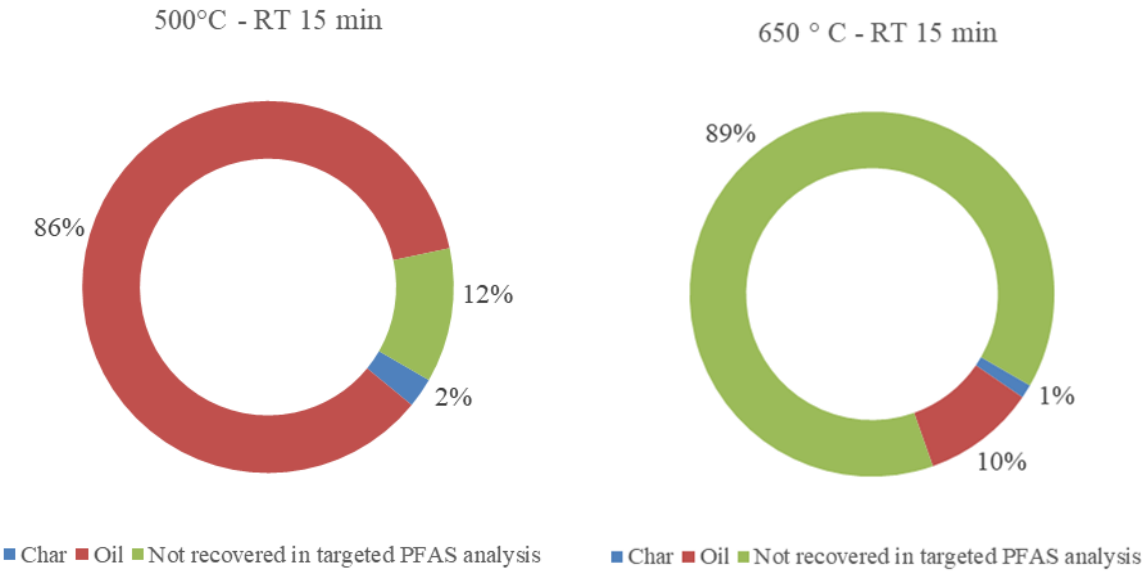

Figure 9.10: Distribution of measurable PFAS-derived fluorine across pyrolysis products (char, oil, and fraction not recovered in targeted PFAS analysis) for pyrolysis at 500 °C and 650 °C with a residence time of 15 minutes.

9.11 Summary of Results

Overall, the results indicate that:

- **Temperature** is the primary driver of PFAS degradation, with efficiencies improving from 95% at 500 °C to 97% at 650 °C.
- **Residence time** had a comparatively minor effect within the tested range (15–30 min), suggesting that PFAS decomposition occurs rapidly once sufficient temperature is reached.
- **$Ca(OH)_2$ addition** further enhanced fluorine removal, reducing F-char to minimal levels and likely promoting CaF_2 formation.
- **Spiking tests** demonstrated near-complete removal (≈99-100%) of PFOS and PFOA, confirming the robustness of the process even under artificially high PFAS concentrations.

Taken together, these findings show that higher temperatures and calcium-based additives produce the "cleanest" char, with minimal fluorine retention and therefore improved suitability for potential land-application scenarios.

9.12 Conclusions

This study investigated the effects of pyrolysis operating conditions and calcium-based additives on product yields, gas composition, and PFAS fate during the thermal treatment of biosolids. Two different feedstocks (Feedstock A and Feedstock B) were tested under controlled conditions, allowing a systematic evaluation of temperature, residence time, and additive effects on both bulk conversion behavior and PFAS removal.

Regarding product yields, pyrolysis temperature was confirmed as the dominant parameter governing mass distribution among char, oil, and gas. Increasing the temperature from 500 to 650 °C resulted in a consistent decrease in char yield and a pronounced increase in gas production for both feedstocks, while liquid yields showed only moderate variations and tended to decrease at higher temperature for Feedstock A. These trends are consistent with enhanced devolatilization and secondary cracking reactions at elevated thermal severity and were in good agreement with literature data. In contrast, solid residence time played a secondary role. Increasing residence time from 15 to 30 min promoted gas formation at 500 °C, but its influence became negligible at 650 °C, indicating that most conversion reactions occur rapidly once sufficient temperature is reached.

Gas composition analysis further highlighted the strong effect of temperature. At 500 °C, the produced gas was dominated by CO_2, with limited formation of reduced species. At 650 °C, the gas composition shifted toward a more reduced mixture, characterized by higher fractions of H_2, CO, and light hydrocarbons, reflecting enhanced cracking and deoxygenation reactions. Time-resolved gas sampling during each run showed only minor variations compared to the temperature effect, confirming that gas composition is primarily controlled by thermal severity rather than sampling time within a single experiment.

PFAS analysis demonstrated that pyrolysis is highly effective in reducing fluorine retention in the solid phase. In non-spiked tests, removal efficiencies were already high under all conditions, increasing from approximately 95% at 500 °C to about 97% at 650 °C. These results indicate that increasing temperature enhances PFAS decomposition and limits fluorine incorporation into the char matrix. The observed temperature-dependent trend is consistent with previous literature findings and confirms temperature as a key controlling factor for PFAS removal.

The addition of calcium hydroxide further improved PFAS removal performance. In both non-spiked and spiked experiments, $Ca(OH)_2$ significantly reduced fluorine retention in the char, leading to removal efficiencies close to 99%. This behavior is consistent with the formation of thermodynamically stable inorganic fluorides, such as CaF_2, which limit fluorine interaction with the carbonaceous matrix and improve the quality of the resulting char.

Spiking experiments with PFOS and PFOA confirmed the robustness of the process under controlled and elevated PFAS loads. Removal efficiencies were consistently near complete (≈99-100%), and residual fluorine levels in char were often comparable to or lower than natural background values. These results demonstrate that pyrolysis under the tested conditions is highly effective in degrading both native and artificially enriched PFAS.

An additional evaluation of the fluorine distribution across pyrolysis products provided further insight into PFAS behavior during thermal treatment. At 500 °C, a larger fraction of measurable PFAS-derived fluorine was associated with the oil fraction, indicating that part of the fluorinated compounds remained within condensable products under moderate thermal conditions. When the temperature increased to 650 °C, the amount of measurable fluorine detected in the oil decreased substantially, while a larger fraction was not recovered in the targeted PFAS analysis. This trend suggests that higher thermal severity promotes the conversion of PFAS into volatile or non-target fluorinated species that are not captured by the targeted analytical method.

Although direct comparisons with literature are limited, as relatively few studies report the distribution of PFAS-derived fluorine across pyrolysis product phases, the observed trend is consistent with the expected increase in PFAS transformation and volatilization at higher temperatures.

Overall, the findings of this work demonstrate that pyrolysis represents an effective treatment strategy for PFAS-contaminated biosolids. Higher temperatures and the use of calcium-based additives produce the

cleanest solid residues, characterized by minimal fluorine retention and improved suitability for downstream management or potential land-application scenarios. Temperature emerges as the primary driver of both product yield distribution and PFAS removal, while residence time plays a secondary role within the investigated range.

References

1. AESAN. (2020). Risk assessment of per- and polyfluoroalkyl substances (PFAS) in food. Spanish Agency for Food Safety and Nutrition. Spanish Agency for Food Safety and Nutrition (AESAN). Questions and answers about PFAS.

2. Ahrens, L. (2011). Polyfluoroalkyl compounds in the aquatic environment: a review of their occurrence and fate. Journal of Environmental Monitoring, 13(1), 20-31. https://doi.org/10.1039/C0EM00373E

3. Alder, A. C., & van der Voet, J. (2015). Occurrence and point source characterization of perfluoroalkyl acids in sewage sludge. *Chemosphere*, *129*, 62-7. https://doi.org/10.1016/j.chemosphere.2014.07.045

4. Allred, B. M., Lang, J. R., Barlaz, M. A., & Field, J. A. (2015). Physical and biological release of poly-and perfluoroalkyl substances (PFASs) from municipal solid waste in anaerobic model landfill reactors. *Environmental science & technology*, *49*(13), 7648-7656. https://doi.org/10.1021/acs.est.5b01040

5. Andreozzi, R. "Advanced oxidation processes (AOP) for water purification and recovery." Catalysis today 53.1 (1999): 51-59.

6. Apedaile, E. (2001)A perspective on biosolids management. *Canadian Journal of Infectious Diseases and Medical Microbiology*, **12**(4), 202–204.

7. Arvaniti, O. S., & Stasinakis, A. S. (2015). Review on the occurrence, fate and removal of perfluorinated compounds during wastewater treatment. *Science of the Total Environment*, *524*, 81-92. https://doi.org/10.1016/j.scitotenv.2015.04.023

8. ASTM International. (2013). ASTM D1762-84: Standard test method for chemical analysis of wood charcoal.

9. Ateia, M., Maroli, A., Tharayil, N., & Karanfil, T. (2019). The overlooked short-and ultrashort-chain poly-and perfluorinated substances: A review. Chemosphere, 220, 866-882.

10. Bach, C. C., Bech, B. H., Brix, N., Nohr, E. A., Bonde, J. P. E., & Henriksen, T. B. (2015). Perfluoroalkyl and polyfluoroalkyl substances and human fetal growth: a systematic review. *Critical reviews in toxicology*, *45*(1), 53-67. https://doi.org/10.3109/10408444.2014.952400

11. Bălan, S. A., Mathrani, V. C., Guo, D. F., & Algazi, A. M. (2021). Regulating PFAS as a chemical class under the California Safer Consumer Products Program. *Environmental health perspectives*, *129*(2), 025001.

12. Ballesteros, V., Costa, O., Iniguez, C., Fletcher, T., Ballester, F., & Lopez-Espinosa, M. J. (2017). Exposure to perfluoroalkyl substances and thyroid function in pregnant women and children: a systematic review of epidemiologic studies. Environment international, 99, 15-28. https://doi.org/10.1016/j.envint.2016.10.015

13. Bamdad, H., Papari, S., Moreside, E., & Berruti, F. (2022). High-temperature pyrolysis for elimination of per-and polyfluoroalkyl substances (PFAS) from biosolids. *Processes*, *10*(11), 2187. https://doi.org/10.3390/pr10112187

14. Barry, V., Winquist, A., & Steenland, K. (2013). Perfluorooctanoic acid (PFOA) exposures and incident cancers among adults living near a chemical plant. *Environmental health perspectives*, *121*(11-12), 1313. https://doi.org/10.1289/ehp.1306615

15. Bräunig, J., Baduel, C., Barnes, C. M., & Mueller, J. F. (2019). Leaching and bioavailability of selected perfluoroalkyl acids (PFAAs) from soil contaminated by firefighting activities. Science of the Total Environment, 646, 471-479. https://doi.org/10.1016/j.scitotenv.2018.07.231

16. Buck, R. C., Franklin, J., Berger, U., Conder, J. M., Cousins, I. T., De Voogt, P., ... & Van Leeuwen, S. P. (2011). Perfluoroalkyl and polyfluoroalkyl substances in the environment: terminology, classification, and origins. Integrated environmental assessment and management, 7(4), 513-541. https://doi.org/10.1002/ieam.258

17. Canadian Council of Ministers of the Environment (CCME). (2012). *Guidelines for the Beneficial Use of Municipal Biosolids*.

18. Canadian Council of Ministers of the Environment. (2012). Canada-wide approach for the management of municipal wastewater biosolids. Winnipeg, MB: CCME.

19. Clarke, B. O., & Smith, S. R. (2011). Review of 'emerging'organic contaminants in biosolids and assessment of international research priorities for the agricultural use of biosolids. *Environment international*, *37*(1), 226-247. https://doi.org/10.1016/j.envint.2010.06.004

20. Coffin, E. S., Reeves, D. M., & Cassidy, D. P. (2023). PFAS in municipal solid waste landfills: Sources, leachate composition, chemical transformations, and future challenges. *Current Opinion in Environmental Science & Health*, *31*, 100418. https://doi.org/10.1016/j.coesh.2022.100418

21. Cogger, C. G., Bary, A. I., Myhre, E. A., & Fortuna, A. M. (2013). Biosolids applications to tall fescue have long-term influence on soil nitrogen, carbon, and phosphorus. *Journal of Environmental Quality*, *42*(2), 516-522. https://doi.org/10.2134/jeq2012.0269

22. Corradini, F., Meza, P., Eguiluz, R., Casado, F., Huerta-Lwanga, E., & Geissen, V. (2019). Evidence of microplastic accumulation in agricultural soils from sewage sludge disposal. Science of the total environment, 671, 411-420. https://doi.org/10.1016/j.scitotenv.2019.03.368

23. Council Directive 86/278/EEC. On the protection of the environment, and in particular of the soil, when sewage sludge is used in agriculture.

24. Council of the European Communities. (1986). Council Directive 86/278/EEC of 12 June 1986 on the protection of the environment, and in particular of the soil, when sewage sludge is used in agriculture. Official Journal of the European Communities, L181, 6–12.

25. de Voogt, P., & Sáez, M. (2006). Analytical chemistry of perfluoroalkylated substances. *TrAC Trends in Analytical Chemistry*, *25*(4), 326-342. https://doi.org/10.1016/j.trac.2005.10.008

26. DeLuca, N. M., Minucci, J. M., Mullikin, A., Slover, R., & Hubal, E. A. C. (2022). Human exposure pathways to poly-and perfluoroalkyl substances (PFAS) from indoor media: A systematic review. Environment international, 162, 107149. https://doi.org/10.1016/j.envint.2022.107149

27. Dewapriya, P., Chadwick, L., Gorji, S. G., Schulze, B., Valsecchi, S., Samanipour, (2023). Per-and polyfluoroalkyl substances (PFAS) in consumer products: Current knowledge and research gaps. *Journal of Hazardous Materials Letters*, *4*, 100086. https://doi.org/10.1016/j.hazl.2023.100086

28. Domingo, J. L., & Nadal, M. (2017). Per-and polyfluoroalkyl substances (PFASs) in food and human dietary intake: a review of the recent scientific literature. Journal of agricultural and food chemistry, 65(3), 533-543.https://doi.org/10.1021/acs.jafc.6b04683

29. EFSA Panel on Contaminants in the Food Chain (EFSA CONTAM Panel), Schrenk, D., Bignami, M., Bodin, L., Chipman, J. K., del Mazo, J., ... & Schwerdtle, T. (2020). Risk to human health related to the presence of perfluoroalkyl substances in food. *Efsa Journal*, *18*(9), e06223. https://doi.org/10.2903/j.efsa.2020.62234

30. Elgarahy, A. M., Eloffy, M. G., Saber, A. N., Abouzid, M., Rashad, E., Ghorab, M. A., ... & Elwakeel, K. Z. (2024). Exploring the sources, occurrence, transformation, toxicity, monitoring, and remediation strategies of per-and polyfluoroalkyl substances: a review. *Environmental Monitoring and Assessment*, *196*(12), 1209.

31. Evich, M. G., Davis, M. J., McCord, J. P., Acrey, B., Awkerman, J. A., Knappe, D. R., ... & Washington, J. W. (2022). Per-and polyfluoroalkyl substances in the environment. Science, 375(6580), eabg9065. DOI:10.1126/science.abg9065

32. Eze, C. G., Okeke, E. S., Nwankwo, C. E., Nyaruaba, R., Anand, U., Okoro, O. J., & Bontempi, E. (2024). Emerging contaminants in food matrices: An overview of the occurrence, pathways, impacts and detection techniques of per-and polyfluoroalkyl substances. Toxicology Reports, 12, 436-447. https://doi.org/10.1016/j.toxrep.2024.03.012

33. Feng, J., Burke, I. T., Chen, X., & Stewart, D. I. (2023). Assessing metal contamination and speciation in sewage sludge: implications for soil application and environmental risk. Reviews in Environmental Science and Bio/Technology, 22(4), 1037-1058. https://doi.org/10.1007/s11157-023-09675-y

34. Fytili, D., & Zabaniotou, A. (2008). Utilization of sewage sludge in EU application of old and new methods—A review. *Renewable and sustainable energy reviews*, *12*(1), 116-140.

35. Gao, N., Quan, C., Liu, B., Li, Z., Wu, C., & Li, A. (2017). Continuous pyrolysis of sewage sludge in a screw-feeding reactor: products characterization and ecological risk assessment of heavy metals. *Energy & Fuels*, *31*(5), 5063-5072. https://doi.org/10.1021/acs.energyfuels.6b03112

36. Gewurtz, S. B., Backus, S. M., De Silva, A. O., Ahrens, L., Armellin, A., Evans, M., ... & Waltho, J. (2013). Perfluoroalkyl acids in the Canadian environment: multi-media assessment of current status and trends. *Environment international*, *59*, 183-200. https://doi.org/10.1016/j.envint.2013.05.008

37. Ghisi, R., Vamerali, T., & Manzetti, S. (2019). Accumulation of perfluorinated alkyl substances (PFAS) in agricultural plants: A review. *Environmental research*, *169*, 326-341. https://doi.org/10.1016/j.envres.2018.10.023

38. Gianico, A., Braguglia, C. M., Gallipoli, A., Montecchio, D., & Mininni, G. (2021). Land application of biosolids in Europe: possibilities, con-straints and future perspectives. Water, 13(1), 103 https://doi.org/10.3390/w13010103

39. Gilmour, J. T., Cogger, C. G., Jacobs, L. W., Evanylo, G. K., & Sullivan, D. M. (2003). Decomposition and plant-available nitrogen in biosolids: Laboratory studies, field studies, and computer simulation. *Journal of Environmental Quality*, *32*(4), 1498-1507. https://doi.org/10.2134/jeq2003.1498

40. Guerra, P., Kim, M., Kinsman, L., Ng, T., Alaee, M., & Smyth, S. A. (2014). Parameters affecting the formation of perfluoroalkyl acids during wastewater treatment. *Journal of Hazardous Materials*, *272*, 148-154. https://doi.org/10.1016/j.jhazmat.2014.03.016

41. Hamid, H., Li, L. Y., & Grace, J. R. (2018). Review of the fate and transformation of per-and polyfluoroalkyl substances (PFASs) in landfills. *Environmental Pollution*, *235*, 74-84. https://doi.org/10.1016/j.envpol.2017.12.030

42. Henze, M., et al. (2008). *Biological Wastewater Treatment*. IWA Publishing.

43. Holder, C., Hubal, E. A. C., Luh, J., Lee, M. G., Melnyk, L. J., & Thomas, K. (2024). Systematic evidence mapping of potential correlates of exposure for per-and poly-fluoroalkyl substances (PFAS) based on measured occurrence in biomatrices and surveys of dietary consumption and product use. International journal of hygiene and environmental health, 259, 114384. https://doi.org/10.1016/j.ijheh.2024.114384

44. Houde, M., De Silva, A. O., Muir, D. C., & Letcher, R. J. (2011). Monitoring of perfluorinated compounds in aquatic biota: an updated review: PFCs in aquatic biota. *Environmental science & technology*, *45*(19), 7962-7973. https://doi.org/10.1021/es104326w

45. Hušek, M., Semerád, J., Skoblia, S., Moško, J., Kukla, J., Beňo, Z., ... & Pohořelý, M. (2024). Removal of per-and polyfluoroalkyl substances and organic fluorine from sewage sludge and sea sand by pyrolysis. Biochar, 6(1), 31. https://doi.org/10.1007/s42773-024-00322-5

46. Inyang, M., Flowers, R., McAvoy, D., & Dickenson, E. (2016). Biotransformation of trace organic compounds by activated sludge from a biological nutrient removal treatment system. *Bioresource technology*, *216*, 778-784. https://doi.org/10.1016/j.biortech.2016.05.124

47. Jahura, F. T., Mazumder, N. U. S., Hossain, M. T., Kasebi, A., Girase, A., & Ormond, R. B. (2024). Exploring the prospects and challenges of fluorine-free firefighting foams (F3) as alternatives to aqueous film-forming foams (AFFF): A review. *ACS omega*, *9*(36), 37430-37444. https://doi.org/10.1021/acsomega.4c03673

48. Jian, J. M., Guo, Y., Zeng, L., Liang-Ying, L., Lu, X., Wang, F., & Zeng, E. Y. (2017). Global distribution of perfluorochemicals (PFCs) in potential human exposure source–a review. Environment international, 108, 51-62. https://doi.org/10.1016/j.envint.2017.07.024

49. Jiang, L., Yao, J., Ren, G., Sheng, N., Guo, Y., Dai, J., & Pan, Y. (2023). Comprehensive profiles of per-and polyfluoroalkyl substances in Chinese and African municipal wastewater treatment plants: New implications for removal efficiency. *Science of The Total Environment*, *857*, 159638. https://doi.org/10.1016/j.scitotenv.2022.159638.

50. Jin, C., Archer, G., & Parker, W. (2018). Current status of sludge processing and biosolids disposition in Ontario. *Resources, Conservation And Recycling*, *137*, 21-31. https://doi.org/10.1016/j.resconrec.2018.05.024

51. Kim, J. H., Ok, Y. S., Choi, G. H., & Park, B. J. (2015). Residual perfluorochemicals in the biochar from sewage sludge. *Chemosphere*, *134*, 435-437. https://doi.org/10.1016/j.chemosphere.2015.05.012

52. Kundu, S., Patel, S., Halder, P., Patel, T., Marzbali, M. H., Pramanik, B. K., ... & Shah, K. (2021). Removal of PFASs from biosolids using a semi-pilot scale pyrolysis reactor and the application of biosolids derived biochar for the removal of PFASs from contaminated water. Environmental Science: Water Research & Technology, 7(3), 638-649. https://doi.org/10.1039/D0EW00763C

53. Kurwadkar, S., Dane, J., Kanel, S. R., Nadagouda, M. N., Cawdrey, R. W., Ambade, B., ... & Wilkin, R. (2022). Per-and polyfluoroalkyl substances in water and wastewater: A critical review of their global occurrence and distribution. *Science of the Total Environment*, *809*, 151003. https://doi.org/10.1016/j.scitotenv.2021.151003

54. Lang, J. R., Allred, B. M., Field, J. A., Levis, J. W., & Barlaz, M. A. (2017). National estimate of per-and polyfluoroalkyl substance (PFAS) release to US municipal landfill leachate. Environmental science & technology, 51(4), 2197-2205. https://doi.org/10.1021/acs.est.6b05005

55. Langberg, H. A., Breedveld, G. D., Kallenborn, R., Ali, A. M., Choyke, S., McDonough, C. A., ... & Hale, S. E. (2024). Human exposure to per-and polyfluoroalkyl substances (PFAS) via the consumption of fish leads to exceedance of safety thresholds. Environment International, 190, 108844. https://doi.org/10.1016/j.envint.2024.108844

56. Lee, H., Tevlin, A. G., Mabury, S. A., & Mabury, S. A. (2014). Fate of polyfluoroalkyl phosphate diesters and their metabolites in biosolids-applied soil: biodegradation and plant uptake in greenhouse and field experiments. *Environmental science & technology*, *48*(1), 340-349. https://doi.org/10.1021/es403949z

57. Liu, Z., McNamara, P., & Zitomer, D. (2017). Autocatalytic pyrolysis of wastewater biosolids for product upgrading. *Environmental Science & Technology*, *51*(17), 9808-9816. https://doi.org/10.1021/acs.est.7b02913

58. Longendyke, G. K., Katel, S., & Wang, Y. (2022). PFAS fate and destruction mechanisms during thermal treatment: a comprehensive review. Environmental Science: Processes & Impacts, 24(2), 196-208. https://doi.org/10.1039/D1EM00465D

59. Mahon, A. M., O'Connell, B., Healy, M. G., O'Connor, I., Officer, R., Nash, R., & Morrison, L. (2017). Microplastics in sewage sludge: effects of treatment. Environmental science & technology, 51(2), 810-818. https://doi.org/10.1021/acs.est.6b04048

60. Malik, P., Nandini, D., & Tripathi, B. P. (2024). Firefighting aqueous film forming foam composition, properties and toxicity: a review. *Environmental Chemistry Letters*, *22*(4), 2013-2033. https://doi.org/10.1007/s10311-024-01739-x

61. Malins, K., Kampars, V., Brinks, J., Neibolte, I., Murnieks, R., & Kampare, R. (2015). Bio-oil from thermo-chemical hydro-liquefaction of wet sewage sludge. *Bioresource Technology*, *187*, 23-29. https://doi.org/10.1016/j.biortech.2015.03.093

62. McDonough, C. A., Li, W., Bischel, H. N., De Silva, A. O., & DeWitt, J. C. (2022). Widening the lens on PFASs: Direct human exposure to perfluoroalkyl acid precursors (pre-PFAAs). Environmental science & technology, 56(10), 6004-6013. https://doi.org/10.1021/acs.est.2c00254

63. Meegoda, J. N., Kewalramani, J. A., Li, B., & Marsh, R. W. (2020). A Review of the Applications, Environmental Release, and Remediation Technologies of Per- and Polyfluoroalkyl Substances. International Journal of Environmental Research and Public Health, 17(21), 8117. https://doi.org/10.3390/ijerph17218117

64. Metcalf & Eddy. (2003). *Wastewater Engineering: Treatment and Reuse*. McGraw-Hill.

65. Metcalf & Eddy. (2007) *Water Reuse*. McGraw-Hill Professional.

66. Mohajerani, A., & Karabatak, B. (2020). Microplastics and pollutants in biosolids have contaminated agricultural soils: An analytical study and a proposal to cease the use of biosolids in farmlands and utilise them in sustainable bricks. Waste Management, 107, 252-265. https://doi.org/10.1016/j.wasman.2020.04.021

67. Moodie, D., Coggan, T., Berry, K., Kolobaric, A., Fernandes, M., Lee, E., ... & Clarke, B. O. (2021). Legacy and emerging per-and polyfluoroalkyl substances (PFASs) in Australian biosolids. *Chemosphere*, *270*, 129143. https://doi.org/10.1016/j.chemosphere.2020.129143

68. Mu, H., Li, J., Chen, L., Hu, H., Wang, J., Gu, C., ... & Wu, B. (2022). Distribution, source and ecological risk of per-and polyfluoroalkyl substances in Chinese municipal wastewater treatment plants. *Environment international*, *167*, 107447. https://doi.org/10.1016/j.envint.2022.107447

69. Müller, C. E., LeFevre, G. H., Timofte, A. E., Hussain, F. A., Sattely, E. S., & Luthy, R. G. (2016). Competing mechanisms for perfluoroalkyl acid accumulation in plants revealed using an Arabidopsis model system. Environmental toxicology and chemistry, 35(5), 1138-1147.https://doi.org/10.1002/etc.3251

70. Navarro, I., De la Torre, A., Sanz, P., Porcel, M. Á., Pro, J., Carbonell, G., & de los Ángeles Martínez, M. (2017). Uptake of perfluoroalkyl substances and halogenated flame retardants by crop plants grown in biosolids-amended soils. Environmental Research, 152, 199-206 https://doi.org/10.1016/j.envres.2016.10.018

71. Ng, C. A., & Hungerbühler, K. (2013). Bioconcentration of perfluorinated alkyl acids: how important is specific binding?. *Environmental science & technology*, *47*(13), 7214-7223.3 DOI: 10.1021/es400981a

72. Nguyen, T. M. H., Bräunig, J., Thompson, K., Thompson, J., Kabiri, S., Navarro, D. A., ... & Mueller, J. F. (2020). Influences of chemical properties, soil properties, and solution pH on soil–water partitioning coefficients of per-and polyfluoroalkyl substances (PFASs). Environmental science & technology, 54(24), 15883-15892. https://doi.org/10.1021/acs.est.0c05705

73. O'Connor, G. A., Elliott, H. A., Basta, N. T., Bastian, R. K., Pierzynski, G. M., Sims, R. C., & Smith, J. E. (2005). Sustainable land application: An overview. *Journal of Environmental Quality*, *34*(1), 7-17.

74. Oun, A., Kumar, A., Harrigan, T., Angelakis, A., & Xagoraraki, I. (2014). Effects of biosolids and manure application on microbial water quality in rural areas in the US. Water, 6(12), 3701-3723. https://doi.org/10.3390/w6123701

75. Phillip, A. (2025). Understanding per-and polyfluoroalkyl substances (PFAS): Environmental persistence, health risks, and regulatory challenges. European Journal of Scientific Research and Reviews, 2(4), 199-211. https://doi.org/10.5455/EJSRR.20250424061440

76. Price, G. W., Astatkie, T., Gillis, J. D., & Liu, K. (2015). Long-term influences on nitrogen dynamics and pH in an acidic sandy soil after single and multi-year applications of alkaline treated biosolids. *Agriculture, Ecosystems & Environment*, *208*, 1-11.

77. Ramírez Carnero, A., Lestido-Cardama, A., Vazquez Loureiro, P., Barbosa-Pereira, L., Rodríguez Bernaldo de Quirós, A., & Sendón, R. (2021). Presence of perfluoroalkyl and polyfluoroalkyl substances (PFAS) in food contact materials (FCM) and its migration to food. Foods, 10(7), 1443. https://doi.org/10.3390/foods10071443

78. Rathnayake, N., Sivaram, A. K., Hakeem, I. G., Pabba, S., Patel, S., Gupta, R., ... & Shah, K. (2025). The fate of per-and polyfluoroalkyl substances (PFAS) during pyrolysis and co-pyrolysis of biosolids with alum sludge and wheat straw. *Journal of Analytical and Applied Pyrolysis*, *187*, 106970. https://doi.org/10.1016/j.jaap.2025.106970

79. Rodowa, A. E., Knappe, D. R., Chiang, S. Y. D., Pohlmann, D., Varley, C., Bodour, A., & Field, J. A. (2020). Pilot scale removal of per-and polyfluoroalkyl substances and precursors from AFFF-impacted groundwater by granular activated carbon. *Environmental Science: Water Research & Technology*, *6*(4), 1083-1094 https://doi.org/10.1039/C9EW00936A

80. Roman-Perez, C. C., Hernandez-Ramirez, G., Kryzanowski, L., Puurveen, D., & Lohstraeter, G. (2021). Greenhouse gas emissions, nitrogen dynamics and barley productivity as impacted by biosolids applications. Agriculture, Ecosystems & Environment, 320, 107577. https://doi.org/10.1016/j.agee.2021.107577

81. Roth, K., Imran, Z., Liu, W., & Petriello, M. C. (2020). Diet as an exposure source and mediator of per-and polyfluoroalkyl substance (PFAS) toxicity. Frontiers in toxicology, 2, 601149. https://doi.org/10.3389/ftox.2020.601149

82. Sasi, P. C., Alinezhad, A., Yao, B., Kubátová, A., Golovko, S. A., Golovko, M. Y., & Xiao, F. (2021). Effect of granular activated carbon and other porous materials on thermal decomposition of per-and polyfluoroalkyl substances: Mechanisms and implications for water purification. *Water Research*, *200*, 117271.

83. Schaider, L. A., Rodgers, K. M., & Rudel, R. A. (2017). Review of organic wastewater compound concentrations and removal in onsite wastewater treatment systems. Environmental science & technology, 51(13), 7304-7317. https://doi.org/10.1021/acs.est.6b04778

84. Schultz, M. M., Higgins, C. P., Huset, C. A., Luthy, R. G., Barofsky, D. F., & Field, J. A. (2006). Fluorochemical mass flows in a municipal wastewater treatment facility. *Environmental science & technology*, *40*(23), 7350-7357.

85. Seiple, T. E., Coleman, A. M., & Skaggs, R. L. (2017). Municipal wastewater sludge as a sustainable bioresource in the United States. Journal of environmental management, 197, 673-680. https://doi.org/10.1016/j.jenvman.2017.04.032

86. Sivaram, A. K., Panneerselvan, L., Surapaneni, A., Lee, E., Kannan, K., & Megharaj, M. (2022). Per-and polyfluoroalkyl substances (PFAS) in commercial composts, garden soils, and potting mixes of Australia. *Environmental Advances*, *7*, 100174 https://doi.org/10.1016/j.envadv.2022.100174

87. Sørmo, E., Castro, G., Hubert, M., Licul-Kucera, V., Quintanilla, M., Asimakopoulos, A. G., ... & Arp, H. P. H. (2023). The decomposition and emission factors of a wide range of PFAS in diverse, contaminated organic waste fractions undergoing dry pyrolysis. *Journal of Hazardous Materials*, *454*, 131447. https://doi.org/10.1016/j.jhazmat.2023.131447

88. Srivastava, P., & Macdonald, B. (2025). PFAS in biosolids: Insights into current and future challenges. Journal of Hazardous Materials Letters, 100163 https://doi.org/10.1016/j.hazl.2025.100163

89. Steenland, K., Fletcher, T., & Savitz, D. A. (2010). Epidemiologic evidence on the health effects of perfluorooctanoic acid (PFOA). *Environmental health perspectives*, *118*(8), 1100. https://doi.org/10.1289/ehp.0901827

90. Sunderland, E. M., Hu, X. C., Dassuncao, C., Tokranov, A. K., Wagner, C. C., & Allen, J. G. (2019). A review of the pathways of human exposure to poly-and perfluoroalkyl substances (PFASs) and present understanding of health effects. *Journal of exposure science & environmental epidemiology*, *29*(2), 131-147. https://doi.org/10.1038/s41370-018-0094-1

91. Tchobanoglous, G., & Leverenz, H. (2013). The rationale for decentralization of wastewater infrastructure. Source separation and decentralization for wastewater management, 101-115.

92. Tchobanoglous, G., Burton, F., Stensel, H., 2003. Metcalf and Eddy Inc., Wastewater Engineering, Treatment and Reuse. McGraw-Hill, New York, NY (US).

93. European Parliament and Council of the European Union. (2020). Directive (EU) 2020/2184 on the quality of water intended for human consumption (Drinking Water Directive). Official Journal of the European Union.

94. U.S. Environmental Protection Agency (EPA), 1993. Standards for the Use or Disposal of Sewage Sludge (40 CFR Part 503). Washington, DC: U.S. Environmental Protection Agency.

95. U.S. Environmental Protection Agency. (2009). Long-chain perfluorinated chemicals (PFCs) action plan.

96. U.S. Environmental Protection Agency. (2024). Method 1633: Analysis of per- and polyfluoroalkyl substances (PFAS) in aqueous, solid, biosolids, and tissue samples by LC–MS/MS (Rev. A). Washington, DC: U.S. EPA.

97. U.S. Food and Drug Administration. (2025). Per- and polyfluoroalkyl substances (PFAS). https://www.fda.gov/food/environmental-contaminants-food/and-polyfluoroalkyl-substances-pfas

98. Venkatesan, A. K., & Halden, R. U. (2013). National inventory of perfluoroalkyl substances in archived US biosolids from the 2001 EPA National Sewage Sludge Survey. Journal of hazardous materials, 252, 413-418 https://doi.org/10.1016/j.jhazmat.2013.03.016

99. Vierke, L., Berger, U., & Cousins, I. T. (2013). Estimation of the acid dissociation constant of perfluoroalkyl carboxylic acids through an experimental investigation of their water-to-air transport. Environmental science & technology, 47(19), 11032-11039. https://doi.org/10.1021/es402691z

100. Walters, E., McClellan, K., & Halden, R. U. (2010). Occurrence and loss over three years of 72 pharmaceuticals and personal care products from biosolids–soil mixtures in outdoor mesocosms. *Water research*, *44*(20), 6011-6020. https://doi.org/10.1016/j.watres.2010.07.051

101. Wang, F., Lu, X., Li, X. Y., & Shih, K. (2015). Effectiveness and mechanisms of defluorination of perfluorinated alkyl substances by calcium compounds during waste thermal treatment. *Environmental science & technology*, *49*(9), 5672-5680. https://doi.org/10.1021/es506234b

102. Wang, F., Shih, K., Lu, X., & Liu, C. (2013). Mineralization behavior of fluorine in perfluorooctanesulfonate (PFOS) during thermal treatment of lime-conditioned sludge. *Environmental science & technology*, *47*(6), 2621-2627.https://doi.org/10.1021/es305352p

103. Wang, Z., Cousins, I. T., Scheringer, M., & Hungerbühler, K. (2013). Fluorinated alternatives to long-chain perfluoroalkyl carboxylic acids (PFCAs), perfluoroalkane sulfonic acids (PFSAs) and their potential precursors. *Environment international*, *60*, 242-248. https://doi.org/10.1016/j.envint.2013.08.021

104. Winchell, L. J., Ross, J. J., Wells, M. J., Fonoll, X., Norton Jr, J. W., & Bell, K. Y. (2021). Per-and polyfluoroalkyl substances thermal destruction at water resource recovery facilities: A state of the science review. Water Environment Research, 93(6), 826-843. https://doi.org/10.1002/wer.1483

105. Wuana, R. A., & Okieimen, F. E. (2011). Heavy metals in contaminated soils: a review of sources, chemistry, risks and best available strategies for remediation. *International Scholarly Research Notices*, *2011*(1), 402647. https://doi.org/10.5402/2011/402647

106. Zhang, J., Gao, L., Bergmann, D., Bulatovic, T., Surapaneni, A., & Gray, S. (2023). Review of influence of critical operation conditions on by-product/intermediate formation during thermal destruction of PFAS in solid/biosolids. *Science of The Total Environment*, *854*, 158796.

Appendix A

Table A.1 - Instrument parameters for the monitored PFAS transitions (MRM)

Abbreviation	Retention time (min)	Precursor ion	Product ion	DP	CE	Quant/qual	Quantification Reference Compound
PFBA	2.299	213.0	169.0	-20	-13	Quant	MPFBA
PFMPA	3.98	229.0	85.0	-25	-17	Quant	M5PFPeA
3:3FTCA	5.065	241.0	177.0	-50	-11	Quant	M5PFPeA
3:3FTCA	5.065	241.0	117.0	-50	-40	Qual	M5PFPeA
PFPeA	5.833	263.0	219.0	-15	-10	Quant	M5PFPeA
PFMBA	6.29	279.0	85.0	-30	-16	Quant	M5PFHxA
4:2FTS	6.843	327.0	307.0	-50	-30	Quant	M242FTS
4:2FTS	6.843	327.0	81.0	-50	-55	Qual	M242FTS
NFDHA	6.956	295.0	201.0	-20	-11	Quant	M5PFHxA
NFDHA	6.956	295.0	85.0	-20	-30	Qual	M5PFHxA
PFBS	7.042	298.9	79.9	-60	-63	Quant	M3PFBS
PFBS	7.042	298.9	98.9	-60	-40	Qual	M3PFBS
PFHxA	7.076	313.0	269.0	-60	-13	Quant	M5PFHxA
PFHxA	7.076	313.0	118.9	-60	-28	Qual	M5PFHxA
HFPO-DA (GenX)	7.359	329.0	185.0	-60	-22	Quant	M3GenX
HFPO-DA (GenX)	7.359	329.0	169.0	-60	-11	Qual	M3GenX
PFEESA	7.486	314.9	135.0	-50	-28	Quant	M5PFHxA
PFEESA	7.486	314.9	83.0	-50	-24	Qual	M5PFHxA
5:3FTCA	7.743	341.0	217.0	-50	-32	Quant	M5PFHxA
5:3FTCA	7.743	341.0	237.0	-50	-18	Qual	M5PFHxA
PFHpA	7.872	363.0	319.0	-40	-14	Quant	M4PFHpA
PFHpA	7.872	363.0	169.0	-40	-22	Qual	M4PFHpA
PFPeS	7.971	348.9	80.0	-70	-70	Quant	M3PFHxS
PFPeS	7.971	348.9	99.0	-70	-70	Qual	M3PFHxS
ADONA	8.115	377.0	251.0	-30	-17	Quant	M3GenX
ADONA	8.115	377.0	84.9	-30	-40	Qual	M3GenX
6:2FTS	8.27	427.0	407.0	-70	-32	Quant	M262FTS
6:2FTS	8.27	427.0	81.0	-70	-65	Qual	M262FTS
PFOA	8.5	413.0	369.0	-20	-14	Quant	M8PFOA
PFOA	8.5	413.0	169.0	-20	-23	Qual	M8PFOA
PFHxS	8.66	398.9	79.7	-90	-87	Quant	M3PFHxS
PFHxS	8.66	398.9	98.9	-90	-75	Qual	M3PFHxS
8:2FTUCA	8.88	457.0	393.0	-15	-15	Quant	M5PFHxA
8:2FTUCA	8.88	457.0	343.0	-15	-50	Qual	M5PFHxA
PFNA	9.06	463.0	419.0	-25	-14	Quant	M9PFNA
PFNA	9.06	463.0	219.0	-25	-24	Qual	M9PFNA
PFHpS	9.26	448.9	80.0	-100	-95	Quant	M8PFOS
PFHpS	9.26	448.9	99.0	-100	-85	Qual	M8PFOS
7:3FTCA	9.29	441.0	317.0	-50	-27	Quant	M5PFHxA
7:3FTCA	9.29	441.0	337.0	-50	-18	Qual	M5PFHxA
8:2FTS	9.36	527.0	507.0	-80	-38	Quant	M282FTS
8:2FTS	9.36	527.0	81.0	-80	-90	Qual	M282FTS
PFDA	9.59	513.0	468.9	-25	-16	Quant	M6PFDA
PFDA	9.59	513.0	219.1	-25	-26	Qual	M6PFDA
PFOS	9.81	498.9	79.9	-50	-110	Quant	M8PFOS
PFOS	9.81	498.9	98.9	-50	-90	Qual	M8PFOS
NEtFOSAA	9.99	584.0	525.9	-60	-30	Quant	d5NEtFOSAA
NEtFOSAA	9.99	584.0	482.9	-60	-22	Qual	d5NEtFOSA
PFUnDA	10.09	563.0	518.9	-20	-17	Quant	M7PFUnDA

PFUnDA	10.09	563.0	269.0	-20	-25	Qual	M7PFUnDA
9Cl-PF3ONS	10.19	530.9	350.9	-50	-40	Quant	M3GenX
9Cl-PF3ONS	10.19	532.9	353.0	-70	-37	Qual	M3GenX
PFNS	10.32	548.9	80.0	-80	-110	Quant	M8PFOS
PFNS	10.32	548.9	99.0	-80	-100	Qual	M8PFOS
NMeFOSAA	9.69	570.0	318.9	-60	-26	Quant	d3NMeFOSAA
NMeFOSAA	9.69	570.0	169.0	-60	-30	Qual	d3NMeFOSAA
PFDoDA	10.55	613.0	568.9	-30	-19	Quant	M2PFDoA
PFDoDA	10.55	613.0	319.0	-30	-26	Qual	M2PFDoA
PFDS	10.782	598.9	80.0	-80	-120	Quant	M8PFOS
PFDS	10.782	598.9	99.0	-80	-110	Qual	M8PFOS
PFTrDA	11.009	662.9	618.9	-40	-17	Quant	M2PFTeDA
PFTrDA	11.009	662.9	169.0	-40	-38	Qual	M2PFTeDA
11Cl-PF3OUdS	11.128	630.9	450.9	-60	-38	Quant	M3GenX
11Cl-PF3OUdS	11.128	632.9	453.0	-70	-41	Qual	M3GenX
PFTeDA	11.441	712.9	668.9	-50	-21	Quant	M2PFTeDA
PFTeDA	11.441	712.9	169.0	-50	-36	Qual	M2PFTeDA
PFDoDS	11.648	698.9	80.0	-80	-130	Quant	M8PFOS
PFDoDS	11.648	698.9	99.0	-80	-140	Qual	M8PFOS
PFOSA	11.735	497.9	78.0	-70	-80	Quant	M8PFOSA
PFOSA	11.735	497.9	169.0	-70	-38	Qual	M8PFOSA
PFHxDA	12.19	812.9	769.0	-50	-18	Quant	M2PFTeDA
PFHxDA	12.19	812.9	169.0	-50	-40	Qual	M2PFTeDA
8:2diPAP	12.242	989.0	543.0	-50	-35	Quant	M2PFTeDA
8:2diPAP	12.242	989.0	79.0	-50	-140	Qual	M2PFTeDA
NMeFOSA	12.761	512.0	169.0	-60	-35	Quant	d3NMeFOSA
NMeFOSA	12.761	512.0	219.0	-60	-33	Qual	d3NMeFOSA
NEtFOSA	13.015	526.0	169.0	-60	-36	Quant	d5NEtFOSA
NEtFOSA	13.015	526.0	219.0	-60	-35	Qual	d5NEtFOSA
MPFBA	2.299	172.0	172.0	-20	-13	EIS	M3PFBA
M5PFPeA	5.833	223.0	223.0	-25	-10	EIS	MPFHxA
M5PFHxA	7.076	273.0	273.0	-20	-13	EIS	MPFHxA
M4PFHpA	7.872	322.0	322.0	-20	-12	EIS	MPFHxA
M8PFOA	8.5	376.0	376.0	-20	-14	EIS	MPFOA
M9PFNA	9.06	427.0	427.0	-20	-14	EIS	MPFNA
M6PFDA	9.59	474.0	474.0	-25	-14	EIS	MPFDA
M7PFUdA	10.09	525.0	525.0	-60	-15	EIS	MPFDA
MPFDoDA	10.55	570.0	570.0	-30	-17	EIS	MPFDA
M2PFTeDA	11.441	670.0	670.0	-40	-21	EIS	MPFDA
M8FOSA	11.735	78.0	78.0	-130	-80	EIS	MPFOS
dNMeFOSA	12.761	169.0	169.0	-100	-34	EIS	MPFOS
dNEtFOSA	13.015	169.0	169.0	-100	-36	EIS	MPFOS
dNMeFOSAA	9.69	419.0	419.0	-50	-28	EIS	MPFOS
dNEtFOSAA	9.99	419.0	419.0	-50	-30	EIS	MPFOS
M3GenX	7.359	169.0	169.0	-40	-10	EIS	MPFOS
M3PFBS	7.042	80.0	80.0	-100	-68	EIS	MPFHxS
M3PFHxS	8.66	80.0	80.0	-120	-85	EIS	MPFHxS
M8PFOS	9.81	80.0	80.0	-150	-110	EIS	MPFOS
M242FTS	6.843	309.0	309.0	-50	-25	EIS	MPFOS
M262FTS	8.27	409.0	409.0	-60	-33	EIS	MPFOS
M282FTS	9.36	509.0	509.0	-100	-37	EIS	MPFOS
M3PFBA	2.299	172.0	172.1	-20	-13	NIS	N/A
MPFHxA	7.076	270.0	270.0	-20	-13	NIS	N/A
MPFOA	8.5	372.0	372.0	-20	-14	NIS	N/A
MPFNA	9.06	423.0	423	-20	-13	NIS	N/A
MPFDA	9.59	470.0	470	-20	-13	NIS	N/A

MPFHxS	8.66	84.0	84	-70	-90	NIS	N/A
MPFOS	9.81	80.0	80	-50	-110	NIS	N/A